An affinity-matured DLL4 ligand for broad-spectrum activation and inhibition of Notch signaling

David Gonzalez-Perez[1], Satyajit Das[2], Elliot Medina[1], Daniel Antfolk[1], Emily D. Egan[3], Stephen C. Blacklow[3], Paulo C. Rodriguez[2], and Vincent C. Luca[1*].

[1] Department of Drug Discovery, Moffitt Cancer Center, Tampa, FL 33602, USA

[2] Department of Immunology, Moffitt Cancer Center, Tampa, FL 33612, USA

[3] Department of Biological Chemistry and Molecular Pharmacology, Harvard Medical School, Boston, Massachusetts 02115; Department of Cancer Biology, Dana Farber Cancer Institute, Boston, Massachusetts 02115, USA

[*] Corresponding author: vince.luca@moffitt.org

Key words: Notch signaling, receptor biology, protein engineering, T cell activation

ABSTRACT

The Notch pathway regulates cell fate decisions and is an emerging target for regenerative and cancer therapies. Recombinant Notch ligands are attractive candidates for modulating Notch signaling; however, their intrinsically low receptor-binding affinity restricts their utility in biomedical applications. To overcome this limitation, we evolved variants of the ligand Delta-like 4 (DLL4) with enhanced affinity and cross-reactivity. A consensus variant with maximized binding affinity, Delta^{MAX}, engages human and murine Notch receptors with 500- to 1000-fold increased affinity compared to wild-type human DLL4. Delta^{MAX} also potently activates human Notch in plate-bound, bead-bound, and cellular formats. When administered as a soluble decoy, Delta^{MAX} inhibits Notch activation in response to either Delta-like (DLL) or Jagged (Jag) ligands, highlighting its utility as both an agonist and antagonist. Finally, we demonstrate that Delta^{MAX} stimulates increased proliferation and expression of effector mediators in primary activated human T cells. Taken together, our data defines Delta^{MAX} as a versatile biotechnological tool for broad-spectrum activation or inhibition of Notch signaling.

32 **INTRODUCTION**

33

34 The Notch pathway is a conserved signaling system that regulates metazoan development and cell
35 fate decisions. In mammals, the core Notch signaling network consists of four Notch receptor
36 paralogs (Notch1-4) and the activating ligands Delta-like 1 (DLL1), Delta-like 4 (DLL4), Jagged1
37 (Jag1), and Jagged2 (Jag2). Notch signaling occurs when cells expressing Notch proteins (signal
38 receivers) interact with adjacent cells expressing DLL or Jag ligands (signal senders)[1–4]. Following
39 ligand engagement, endocytosis of the DLL or Jag protein into the sender cell exerts a "pulling"
40 force that destabilizes the negative regulatory region (NRR) of the Notch extracellular domain
41 (ECD)[5,6]. This mechanical tension exposes a proteolytic cleavage site (S2) that is processed by the
42 ADAM10 metalloprotease[7,8]. ADAM10 cleavage results in the shedding of the Notch ECD, which
43 in turn sensitizes the Notch transmembrane domain to cleavage by the intramembrane protease
44 gamma-secretase[1,9,10]. This second proteolytic event releases the Notch intracellular domain
45 (NICD) from the plasma membrane and it translocates to the nucleus to serve as a transcriptional
46 cofactor[1,2,11].

47

48 Notch extracellular domains (ECDs) are comprised of 29 to 36 epidermal growth factor (EGF)
49 domains and the juxtamembrane negative regulatory region (NRR). Ligand ECDs also have a
50 modular structure and contain an N-terminal C2-like (MNNL) domain, a Delta/Serrate/Lag3
51 (DSL) domain, 6 to 16 EGF domains, and a cysteine rich domain that is only present in Jag
52 proteins. Through structural, biochemical, and cell-based studies, we and others have determined
53 that the C2, DSL, and EGF1-3 region of DLL or Jag engage five centrally positioned Notch EGF
54 domains (EGF8-12 in Notch1) to initiate signaling[4,12–15]. Interactions between Notch and ligand
55 ECDs are low affinity[4,13,16], and co-crystallization of rat DLL4:Notch1 and Jag1:Notch1
56 complexes required the incorporation of affinity-enhancing mutations into the ligands[14,15]. Despite
57 the low affinity of receptor for ligand, Notch signaling occurs productively *in vivo*, because
58 receptor-ligand interactions may be strengthened by catch bond formation or multivalent
59 binding[15,17–19].

60

61 Although the Notch transcriptional machinery is broadly conserved, preferential interactions have
62 been described between receptor and ligand subtypes[1]. For example, DLL4 is a higher affinity

63 ligand for Notch1 than is DLL1[13], while DLL1 activates Notch1 and Notch2 roughly
64 equivalently[16]. Signaling through specific Notch-ligand pairs is also associated with distinct
65 functional outcomes. During angiogenesis, Notch1:DLL4 interactions inhibit tip sprouting and
66 Notch1:Jag1 interactions promote vessel growth[20], and Jagged2:Notch3 interactions stimulate the
67 differentiation of γ/δ T cells[21]. Comparative studies have begun to identify differences in the
68 structures[15], binding affinities[13], and signaling dynamics[19] of selected ligands that may contribute
69 to their unique functional properties. However, the precise molecular mechanisms controlling
70 receptor- and ligand-specific signaling remain unclear.
71
72 Depending on cellular context, Notch signaling may induce the differentiation or proliferation of
73 stem cells, and the broad influence of Notch on stem cell behavior has made the pathway an
74 attractive target for regenerative therapeutics. Moreover, Notch signaling has been shown to have
75 context-dependent tumor suppressor or oncogenic functions in human cancers[22]. The pleiotropic
76 effects of Notch signaling suggest that both agonists and antagonists of Notch signaling will be
77 valuable for biomedical applications. Several antagonists are currently in clinical trials for the
78 treatment of cancer, including gamma-secretase inhibitors and monoclonal antibodies targeting
79 individual Notch ECDs [23–25]. On the other hand, the development of Notch agonists has been
80 challenging because soluble drugs cannot exert the mechanical force necessary for receptor
81 activation. Thus far, a single agonist antibody has been described for Notch3, which may be
82 uniquely susceptible to antibody-mediated activation due to the inherent instability of the Notch3
83 NRR[26,27].
84
85 Recombinant DLL or Jag ECDs are attractive "one-size-fits-all" candidates for activating or
86 inhibiting Notch signaling. In their soluble form, ligand ECDs act as untethered decoys that bind
87 to Notch receptors and inhibit ligand-mediated activation. The on-target specificity of ligand ECDs
88 may also be advantageous given that gamma-secretase cleaves a myriad of cellular substrates that
89 are unrelated to the Notch pathway[28]. Alternatively, surface- or matrix-tethered DLL or Jag ligands
90 stimulate Notch signaling, presumably because immobilization provides sufficient resistance force
91 for receptor activation. Despite their potential to function as universal modulators of the Notch
92 pathway, the intrinsically low affinities of DLL and Jag ligands limits their practical utility as

93 biomedical tools. Additionally, the preferential binding observed between certain receptor:ligand
94 pairs may restrict the activity of a given ligand to a subset of Notch paralogs.
95
96 To overcome the biochemical limitations of endogenous Notch ligands, we used yeast display and
97 mutational engraftment to engineer potent, broadly-reactive human DLL4 variants. By combining
98 mutations from multiple directed evolution campaigns, we developed a consensus variant, named
99 Delta^{MAX}, that binds with greatly enhanced affinity to human and murine Notch receptor paralogs.
100 We determined that Delta^{MAX} is a more potent Notch activator than WT DLL4 in several
101 commonly used ligand-presentation formats, and that the proliferation and expression of effector
102 mediators in primary T cells is enhanced following conditioning stimulation with Delta^{MAX}.
103 Furthermore, the soluble Delta^{MAX} ECD functions as a potent, "pan-Notch" inhibitor by competing
104 for the Notch ligand-binding site. Our collective insights demonstrate that affinity-matured Notch
105 ligands are highly-effective, multifunctional tools for modulating Notch signaling.
106
107 **RESULTS**
108 **Structure-guided engineering of high-affinity DLL4 variants.** We employed a structure-guided
109 engineering strategy to evolve broadly-reactive, high-affinity DLL4 variants. Crystal structures of
110 DLL4:Notch1 and Jag1:Notch1 complexes revealed that the ligand C2 and DSL domains engage
111 the Notch1 EGF12 and EGF11 domains, respectively. In each of these structures, the C2:EGF12
112 interface was named Site 1 and the DSL:EGF11 interface was named Site 2. However, an
113 additional "Site 3" binding interface was also visualized in the Jag1:Notch1 structure and forms
114 between Jag1 EGF1-3 and Notch1 EGF8-10[14,15]. Solution binding studies demonstrated that Site
115 3 contributes substantially to Jag1:Notch1 interactions, but has a minimal effect on DLL4:Notch1
116 interactions[15]. Therefore, we designed a site-directed mutant library to select for DLL4 mutations
117 that recapitulate the Site 3 interaction observed in Notch1:Jag1. The library was generated by
118 varying nine DLL4 residues (H256, N257, T271, L279, F280, T289, S301, N302, Q305) that were
119 analogous to Site 3 interface residues in Jag1 EGF2 and EGF3. We employed a "light mutagenesis"
120 approach in which each interface residue was allowed to encode for the WT DLL4 residue, the
121 equivalent Jag1 residue, or biochemically similar residues (Fig. 1a, 1b).
122

123 We used yeast display to select high-affinity Notch binders from our DLL4 mutant library (Fig.
124 1b). The library was stained with Notch1 or Notch3 ECD constructs containing the ligand-binding
125 domains (Notch1 EGF8-12, Notch3 EGF5-12) and several rounds of selections were performed to
126 isolate high-affinity binders. The Notch3-selected yeast had the greatest enrichment of Notch-
127 binders, and sequencing of individual colonies revealed twenty-one different mutations at interface
128 positions (Fig. 1c, Extended Data Fig. 1). A clone containing five mutations (N257P, T271L,
129 F280Y, S301R, and Q305P) was overrepresented in the samples and was selected for further
130 characterization. This clone is henceforth referred to as DLL4.v2. Analysis of the DLL4.v2
131 sequence revealed that F280Y and S301R are novel mutations that are not present in other
132 mammalian Notch ligands (Extended Data Fig. 2), and that N257P, T271L, and Q305P had
133 converted to the Jag1 residues. The other four mutated positions (DLL4 residues H256, L279,
134 T289, and N302) reverted to the wild-type sequence (Fig. 1c). Notably, N257P was previously
135 introduced into DLL4 to recreate the "DOS motif" found in Jag1[2,29], and this substitution increased
136 receptor binding and signaling[30].
137
138 We analyzed the DLL4.v2 mutations in the context of Site 3 of the Notch1:Jag1 complex structure
139 to gain insight into their mechanisms of affinity-enhancement (Fig. 1d, Extended Data Fig. 3).
140 Based on this analysis, we predict that the N257P, T271L, and Q305P mutations enhance binding
141 by improving hydrophobic packing at the binding interface (Extended Data Fig. 3a, 3b, 3c). The
142 F280Y mutation may stabilize the overall fold of the DLL4 protein by replacing the exposed
143 hydrophobic Phe^{280} phenyl group with a more hydrophilic tyrosyl group (Extended Data Fig. 3d).
144 Lastly, we predict that S301R enhances binding by introducing contacts between the guanidinium
145 group of DLL4 Arg^{301} and the main-chain carbonyl of the Notch1 Cys^{321} and/or the aliphatic side
146 chain of Val^{322} (Extended Data Fig. 3e).
147
148 **Generation of a high-affinity DLL4 consensus variant.** We combined multiple sets of affinity-
149 enhancing mutations in an attempt to engineer a DLL4 protein with maximal receptor-binding
150 affinity. We used the high-affinity DLL4.v2 variant as a starting point for our construct design.
151 We then engrafted five affinity-enhancing mutations (G28S, F107L, N118I, H194Y, and L206P)
152 from our previously reported rat DLL4 variant (E12)[14] onto the human DLL4.v2 scaffold (Fig.
153 2a). As the E12 mutations are located within the C2 and DSL domains (Site 1 and Site 2) of DLL4,

154 we hypothesized that they would have an additive or synergistic effect when combined with the
155 Site 3 mutations of DLL4.v2. The resulting consensus variant, Delta^{MAX}, contains 10 total
156 mutations: G28S, F107L, N118I, H194Y, L206P, N257P, T271L, F280Y, S301R, and Q305P (Fig.
157 2a).
158
159 **DLL4 variants bind to human and mouse Notch receptors with high-affinity.** We used surface
160 plasmon resonance (SPR) to determine the binding affinity between Delta^{MAX} and the ligand-
161 binding regions of Notch1-4. As a basis for comparison, we also generated a WT DLL4 construct,
162 a DLL4.v2 construct, and a "DLL4.v1" construct containing the five E12 mutations (G28S, F107L,
163 N118I, H194Y, and L206P) (Fig. 2a, Extended Data Fig. 4). Analysis of the SPR data revealed
164 that DLL4.v1, DLL4.v2, and Delta^{MAX} bound to all four human Notch receptors with enhanced
165 affinity compared to WT DLL4 (Fig. 2b). DLL4.v1 bound to Notch1-4 with 70 to 200-fold
166 increased affinity depending on the receptor subtype, and DLL4.v2 bound to Notch1-4 with 6 to
167 28-fold higher affinity. The larger contribution of Site 1 and Site 2 mutations from E12 to the
168 interaction is consistent with previous data indicating that the C2 and DSL domains form the
169 dominant receptor-binding interface. Delta^{MAX} bound to Notch1 with a dissociation constant (K_D)
170 of 24 nM, Notch2 with a K_D of 54 nM, Notch3 with a K_D of 49 nM, and Notch4 with a K_D of 24
171 nM. Compared to WT DLL4, the nanomolar affinity interactions between Delta^{MAX} and Notch1-
172 4 represent enhancements of 1,100-fold, 670-fold, 591-fold, and 532-fold, respectively.
173
174 In addition to human Notch1-4, we measured the binding affinity between each DLL4 variant and
175 the EGF6-13 region of murine Notch1 (mNotch1 EGF6-13) to test for cross-species reactivity
176 (Fig. 2b, Extended Data Fig. 4, 5). Each ligand bound to murine Notch1 and human Notch1 with
177 comparable affinities, and Delta^{MAX} bound to mNotch1 EGF6-13 with a K_D of 24 nM, which is
178 nearly identical to its affinity for human Notch1 (24 nM K_D). We attempted to fit the SPR data to
179 compare the kinetic binding parameters between Notch and each of the four DLL4 constructs. The
180 rapid dissociation of WT DLL4 precluded kinetic fitting of the binding data, however, visual
181 inspection of the SPR sensograms indicates that the increasing affinities of DLL4.v1, DLL4.v2,
182 and Delta^{MAX} are linked to progressive decreases in off-rate (Fig. 2c).
183

184 **Delta^{MAX} has improved expression and thermostability.** We also tested whether the affinity-
185 enhancing mutations impacted the expression and stability of the Delta^{MAX} protein. We performed
186 a thermal denaturation experiment using differential scanning fluorimetry (DSF) to compare the
187 melting temperatures of WT DLL4 and Delta^{MAX}. We determined that the melting temperature
188 (T_m) of WT DLL4 was 47 ºC and that the T_m of Delta^{MAX} was increased by 11 ºC to 58 ºC (Fig.
189 2d). Furthermore, expression yield of the Delta^{MAX} protein was increased by 2-fold compared to
190 WT DLL4 (Extended Data Fig. 4g). Taken together, our SPR and DSF measurements indicate that
191 Delta^{MAX} exhibits enhanced affinity, stability and expression while maintaining a broad reactivity
192 profile against human and murine Notch receptors.
193
194 **Delta^{MAX} activates Notch more potently than WT DLL4.** We performed a series of signaling
195 assays to evaluate the Notch activation potency, signaling kinetics, and cross-reactivity of our
196 high-affinity Delta^{MAX} ligand. We first characterized the signaling potency of Delta^{MAX} protein
197 using fluorescent (H2B-Citrine) Notch1 reporter cells (Extended Data Fig. 6a, 7a)[31]. As our goal
198 was to develop an accessible tool for modulating Notch activity, we performed this assay by non-
199 specifically adsorbing DLL4 proteins to 96-well tissue culture plates. This facile method requires
200 minimal manipulation of proteins and is an established method for stimulating Notch activation *in*
201 *vitro*. Plates were coated with various concentrations of WT DLL4 or Delta^{MAX} and Notch1
202 reporter cells were cultured on the ligand-coated surfaces. After 24 hours, fluorescence was
203 monitored by flow cytometry. Fitting the data revealed that EC50 values for Notch1 activation by
204 WT DLL4 and Delta^{MAX} were 1.7 μM and 6.8 nM, respectively, which corresponds to a 250-fold
205 improvement in Notch activation efficiency (Fig. 3a). Moreover, the E_{max} induced by Delta^{MAX}
206 was 20% greater than that induced by WT DLL4, indicating that Delta^{MAX} is capable of activating
207 Notch signaling with greater amplitude and potency than WT DLL4.
208
209 We next tested whether C-terminal anchoring of DLL4 proteins improves signaling output. This
210 strategy mimics the orientation the proteins adopt on the cell surface and was achieved by
211 biotinylating the ligand C-termini prior to attachment to streptavidin-coated plates. For both WT
212 DLL4 and Delta^{MAX}, oriented coupling induced a higher maximum level of Notch1 activation than
213 non-specific adsorption (Fig. 3b). In this format, Delta^{MAX} was also more potent than WT DLL4
214 and activated Notch1 with an EC50 of 1.7 nM compared to 16 nM for WT DLL4. We also

215 performed a time-course experiment to evaluate the signaling kinetics of Delta^{MAX}. We determined
216 that Delta^{MAX} activates Notch1 more rapidly than WT DLL4, and that this effect is most
217 pronounced in the first 4 to 8 hours following ligand stimulation (Fig. 3c). These findings indicate
218 that the high-affinity Delta^{MAX} ligand potently activates Notch regardless of coupling strategy, and
219 that oriented coupling maximizes the efficiency of Notch activation through DLL4 ligands.
220
221 **Delta^{MAX} strongly activates multiple human Notch receptors.** We tested the ability of Delta^{MAX}
222 to activate different human Notch receptor subtypes using an established luciferase reporter assay.
223 For this assay, we used U2OS cells stably expressing chimeric Notch1, Notch2, or Notch3 proteins
224 (Extended Data Fig. 6b)[32]. Notch4 was excluded from our study since it has been suggested that
225 Notch4 inhibits signaling and it is not responsive to ligand-mediated activation *in vitro*[33]. To
226 compare the signaling of each ligand, we cultured Notch1, Notch2, and Notch3 reporter cells with
227 C-terminally anchored WT DLL4 or high-affinity Delta^{MAX} (Fig 3d). When we stimulated Notch1
228 cells with WT DLL4, we observed a dose-dependent increase in Notch signaling. The Delta^{MAX}
229 variant more potently activated Notch1 across all concentrations and induced 2-fold higher levels
230 of Notch1 signaling relative to WT DLL4 at the highest concentration tested (50 nM). Delta^{MAX}
231 also activated Notch2 and Notch3 more potently than WT DLL4. For Notch2 and Notch3, relative
232 Delta^{MAX} signaling was increased by 2.5-fold and 3-fold, respectively. These functional data
233 indicate that enhanced affinity of Delta^{MAX} leads to increased signaling through Notch1-3, and that
234 Delta^{MAX} is a viable tool for potently activating multiple human Notch receptors.
235
236 To determine whether Delta^{MAX} stimulates increased activation in cells expressing endogenous
237 levels of Notch1, we compared the signaling of Delta^{MAX} and WT DLL4 in U2OS (osteosarcoma
238 epithelial) cells and MCF-7 (breast cancer). U2OS and MCF-7 cells were each stimulated for 24
239 hours using C-terminally anchored WT DLL4 and Delta^{MAX} and Notch1 activation was detected
240 by Western blotting for the cleaved Notch1 ICD (Fig. 3e). We found that Delta^{MAX} activated Notch
241 signaling much more potently than WT DLL4 in both cell lines, indicating that Delta^{MAX} is a more
242 potent ligand regardless of Notch expression level.
243
244 Thus far, all our signaling assays were performed using purified recombinant ligands. To evaluate
245 the potency of Delta^{MAX} when expressed as a full-length transmembrane protein in cells, we

246 performed a co-culture Notch signaling assay. We generated HEK293T cell lines stably expressing
247 either full-length WT DLL4 or Delta^{MAX} (Extended Data Fig. 7b) and then co-cultured the ligand-
248 expressing cells with Notch1, Notch2, or Notch3 reporter cells (Extended Data Fig. 6b) at a 1:1
249 ratio. In this co-culture format, we determined that the E_{max} of Delta^{MAX} signaling through Notch1
250 and Notch3 was ~2-fold higher than WT DLL4. The luciferase signal for Notch2 was low for both
251 ligands, although only Delta^{MAX} induced a significant level of Notch2 activation compared to
252 unstimulated cells (P = 0.037) (Fig. 3f).
253
254 **Comparison of Delta^{MAX} signaling on plates, beads, and cells.** A myriad of ligand-presentation
255 platforms have been developed to activate mechanosensitive Notch receptors, including ligand-
256 coated plates, ligand-coated beads, antibody-clustered ligands, ligand-infused matrices, and
257 ligand-overexpressing stromal cell lines[13,14,18,30,34–36]. To our knowledge, no single experiment has
258 directly compared the level of Notch signaling induced across different ligand-presentation
259 formats. Here, we compared the signaling of Delta^{MAX} in five different formats to determine an
260 optimal strategy for maximizing Notch activation. Fluorescent Notch1 reporter cells were cultured
261 with yeast-displayed Delta^{MAX}, 293T cells-expressing Delta^{MAX}, Delta^{MAX}-coated microbeads,
262 plates coated adsorbed with Delta^{MAX} (non-specific coupling), and streptavidin plates coated with
263 C-terminally biotinylated Delta^{MAX} (oriented coupling) (Fig. 3g, Extended Data Fig. 8). We
264 determined that yeast-displayed Delta^{MAX} did not induce a significant change in Notch1 activation,
265 which may be due to the inability of cell wall-tethered ligands to undergo endocytosis, or because
266 the low mass of the yeast cells provides insufficient resistance. However, the remaining formats
267 induced 15- to 50-fold increases in Notch1 activation relative to controls. The co-culture method
268 induced the lowest level of Notch1 activation (15-fold), followed by Delta^{MAX}-coated beads (21-
269 fold), non-specific adsorption (23-fold), and oriented coupling (50-fold) (Fig. 3g). Taken together,
270 our data reveal that recombinant protein-based formats (plate- or bead-bound ligands) induced
271 higher levels signaling than cell-based methods. Furthermore, the increased E_{max} of C-terminally
272 anchored Delta^{MAX} suggests that the greater accessibility of the ligand-binding C2-EGF3 domains
273 is optimal for maximal Notch stimulation.
274
275 **Soluble Delta^{MAX} is a potent pan-Notch inhibitor.** In the absence of membrane anchor, DLL4
276 ECDs are predicted to block ligand-mediated Notch activation by functioning as soluble decoys.

277 However, WT DLL4 binds to human Notch receptors with micromolar affinities that fall outside
278 of the expected range for effective pharmacological inhibition. We hypothesized that our high-
279 affinity DLL4 variants would overcome the affinity-limitations of WT DLL4 to function as potent
280 Notch antagonists. To test this hypothesis, we cultured fluorescent Notch1 reporter cells on C-
281 terminally anchored WT DLL4-coated plates in the presence of soluble competitors. We added
282 increasing concentrations of soluble WT DLL4, DLL4.v1, DLL4.v2, and Delta^{MAX} ECDs to the
283 cells and then monitored reporter signal after 24 hours. We determined that, among the four
284 proteins, only soluble Delta^{MAX} was able to efficiently block plate-bound WT DLL4-induced
285 Notch1 activation and inhibited signaling with an IC50 of 0.6 nM. By contrast, administration of
286 soluble WT DLL4 only reduced reporter activity by ~25% at the highest concentration tested (300
287 nM). DLL4.v1 and DLL4.v2 were more potent inhibitors than WT DLL4, but less potent than
288 Delta^{MAX}, and neither DLL4.v1 or DLL4.v2 fully blocked Notch1 activation (Fig. 4a).
289
290 Most small molecule Notch inhibitors are non-specific and target multifunctional ADAM10/17 or
291 gamma-secretase proteases required for Notch activation. Therefore, we compared the inhibition
292 potency of our Notch-selective Delta^{MAX} protein to the established gamma-secretase inhibitor
293 DAPT and BB-94, a broad-spectrum metalloprotease inhibitor, BB-94 that inhibits ADAM10 (Fig.
294 4b). We determined that Delta^{MAX} inhibited Notch1 activation with an IC50 of 1 nM, which was
295 40-fold more potent than DAPT (IC50 of 40 nM) and 1000-fold more potent than BB-94 (IC50 of
296 1000 nM). We also compared the inhibition of Delta^{MAX} and DAPT in a co-culture assay. Both
297 DAPT and Delta^{MAX} inhibited cellular DLL4 less potently than plate-bound DLL4, and the IC50
298 of DAPT and Delta^{MAX} were 100 and 400 nM, respectively (Extended Data Fig. 9). Thus, Delta^{MAX}
299 functions as a potent and selective inhibitor of ligand-mediated Notch signaling, and the potency
300 of inhibition depends on the format in which the wild-type ligand is presented.
301
302 We also tested the ability of Delta^{MAX} to inhibit signaling by ligands other than DLL4. First, we
303 generated stable HEK293T cell lines expressing DLL1, DLL4, Jag1, and Jag2 and confirmed
304 ligand-expression levels by antibody staining (Extended Data Fig. 10). We then co-cultured DLL1,
305 DLL4, Jag1 or Jag2 cells with Notch3 luciferase reporter cells that were pre-mixed with a constant
306 (3 μM) concentration of soluble WT DLL4 or Delta^{MAX} (Fig. 4c). We determined that Delta^{MAX}
307 effectively inhibited productive signaling by DLL1, DLL4, Jag1, and Jag2, with a reduction in

308 reporter signal ranging from 70-85%. On the other hand, WT DLL4 only weakly inhibited Notch
309 activation through the four ligands, reducing reporter signal by 10-40%.
310
311 Lastly, we assessed whether Delta^{MAX} could inhibit signaling through different human Notch
312 paralogs. We incubated Notch1, Notch2 and Notch3 luciferase reporter cell lines with various
313 concentrations of soluble WT DLL4 or Delta^{MAX}, and then cultured the cells on plates coated with
314 DLL4-coated plates to monitor Notch activation (Fig. 4d). We determined that addition of the
315 Delta^{MAX} competitor led to dose-dependent decreases in signaling for Notch1, Notch2, and
316 Notch3, and that WT DLL4 did not significantly inhibit Notch activation at all concentrations
317 tested.
318
319 **Delta^{MAX} increased human CD8^{+} T cell proliferation and effector markers.** Notch signaling
320 contributes to several aspects of immunobiology and influences the proliferation, differentiation,
321 and antitumor function of CD8^{+} T cells[37–41]. Therefore, we developed an assay to test the effect of
322 Delta^{MAX} on activated T cells (Fig. 5a). As stromal cells are an established platform for Notch
323 stimulation in T cells, we generated artificial antigen presenting K562 cells (aAPCs) expressing
324 the Fc receptor CD32 (renamed K32 cells), and similar surface levels of WT DLL4 or Delta^{MAX}
325 (Fig. 5b)[42]. We then co-cultured these ligand-expressing cells with primary T cells in the presence
326 of increasing concentrations of the T cell-activating antibody OKT3. CD32 expression enabled
327 OKT3 Fc binding to K32 cells and subsequent CD3-TCR activation on T cells. Human CD8^{+} T
328 cells were negatively isolated from peripheral blood and co-cultured with K32 cells pre-loaded
329 with increasing concentrations of OKT3 to analyze T cell proliferation and IFNγ secretion (Fig.
330 5c, 5d). Delta^{MAX} treatment enhanced the percentage of proliferating CD8^{+} T cells between 27%
331 and 15% along the OKT3 concentrations assayed (P = 0.032), while WT DLL4 did not show a
332 significant improvement over the stimulation with K32 cells lacking DLL4 ligands (mock) (Fig.
333 5c). Additionally, Delta^{MAX} increased IFNγ secretion from CD8^{+} T cells 10-15% compared with
334 WT DLL4 treatment (P = 0.047) (Fig. 5d).
335
336 Next, we used RT-PCR to quantify the mRNA levels of Notch and T cell effector related markers
337 over four days of CD8^{+} T cell stimulation with K32 loaded with 0.0125 μg/mL OKT3. We
338 determined that Delta^{MAX}-stimulated T cells had increased levels of effector mediators IFNγ and

339 Granzyme B, as well as elevated expression of Notch target Hes-4 compared to counterparts
340 conditioned with WT DLL4 or mock (Fig. 5e). Lastly, we performed a western blot analysis to
341 compare Notch1 and Notch2 activation in T cells that were stimulated with WT DLL4 or Delta^{MAX}.
342 Using an antibody to the cleaved Notch1 or Notch2 ICD, we determined that activation of both
343 Notch1 and Notch2 was increased for Delta^{MAX}-treated cells relative to WT DLL4, and the
344 difference in Notch2 activation was more prominent than that of Notch1 (Fig. 5f). Thus, results
345 show the promotion of CD8^{+} T cell function induced by aAPCs expressing Delta^{MAX}.
346
347 **DISCUSSION**
348 Recombinant DLL and Jag ligand ECDs bind weakly to Notch receptors and are inefficient
349 modulators of Notch signaling. We engineered the synthetic Delta^{MAX} ligand to be a versatile tool
350 for activating or inhibiting mammalian Notch receptors, depending on the manner in which it is
351 administered. Compared to WT DLL4, immobilized or cellular Delta^{MAX} exhibits varying degrees
352 of increased signaling potency, and soluble Delta^{MAX} functioned as a Notch-specific inhibitor
353 when administered as a soluble decoy. Furthermore, the increased thermostability (ΔT_m 11°C) and
354 expression (2-fold higher yield) of Delta^{MAX} are both favorable properties for protein biologics.
355
356 Our functional studies revealed that Delta^{MAX} activates Notch more potently than WT DLL4 in
357 plate-bound, bead-bound, and cellular formats. Among the methods tested, we determined that C-
358 terminally anchored Delta^{MAX} induced the highest levels of Notch signaling, followed by non-
359 specifically adsorbed ligands, ligand-coated beads, and cellular ligands. The largest difference in
360 signaling potency between WT DLL4 and Delta^{MAX} was observed when ligands were non-
361 specifically adsorbed to plastic. The WT DLL4 protein was a poor Notch activator in this format
362 (EC50 1.7 μM), while Delta^{MAX} was remarkably potent (EC50 6.8 nM). The strong signaling
363 activity can enable entire flasks or tissue culture plates to be pre-conditioned with Delta^{MAX} as a
364 high-throughput means of activating Notch in cultured cells. Furthermore, non-specific adsorption
365 requires low quantities of protein and can be performed with unmodified ligand ECDs, making
366 this method highly accessible for a wide range of biotechnological applications.
367
368 Soluble DLL4 ECDs do not activate Notch because they are unable to exert the requisite pulling
369 force. Instead, these ECD are predicted to inhibit signaling by competing for the ligand-binding

370 site on the Notch receptor. We demonstrated that, even at high-concentrations, the micromolar
371 binding affinity of WT DLL4 prevents it from functioning as an effective Notch antagonist. On
372 the other hand, Delta^{MAX} potently inhibited Notch activation by all four activating ligands (DLL1,
373 DLL4, Jag1, and Jag2). The broad-reactivity profile of Delta^{MAX} also enabled it to inhibit ligand-
374 mediated activation of Notch1, Notch2, and Notch3. Current strategies for pan-Notch inhibition
375 require the use of gamma-secretase or ADAM10/17 inhibitors, which block the cleavage of
376 numerous cellular substrates in addition to Notch. Alternatively, antibodies targeting the NRR
377 domain have been used to block signaling by individual Notch receptor subtypes. We found that
378 Delta^{MAX} inhibited Notch signaling with similar potency to the established gamma-secretase
379 inhibitor DAPT. Therefore, this ability of Delta^{MAX} to block signaling by all Notch receptors
380 makes it a unique pharmacological tool as a highly selective, pan-Notch inhibitor.
381
382 Notch signaling is central regulator of T cell biology and influences T cell activation, proliferation,
383 and cytolytic effector functions[37–40,43,44]. We previously demonstrated that constitutive Notch
384 activation by overexpression of NICD enhances the antitumor activity of adoptively transferred
385 murine CD8^{+} T cells[45]. As this method required genetic modification of the T cells, we aimed to
386 develop an *ex vivo* platform for transient Notch activation using Delta^{MAX}. In the present study,
387 we determined that co-culturing activated T cells with K32 cells expressing Delta^{MAX} induces
388 increased T cell proliferation and expression of effector mediators compared to co-culture with
389 WT DLL4. This approach could be potentially beneficial for strategies of expansion of anti-tumor
390 CAR-T or TILS for further adoptive transfer by triggering Notch-related metabolic and anti-tumor
391 signals.
392
393 Various ligand presentation strategies have been developed for activating Notch in T cells, and in
394 these systems, the dosage of Notch signaling has proven to be important for achieving optimal
395 outcomes. For example, low doses of DLL1 stimulate the differentiation of hematopoietic stem
396 and progenitor cells (HSPCs) into mixed populations of lymphoid and myeloid precursors,
397 whereas high-doses promote the differentiation of only lymphoid precursors[46]. Additionally,
398 stromal cells that express DLL4, which binds to Notch1 with higher affinity than DLL1[13], more
399 efficiently drives T cell lymphopoiesis[35]. Given the tunable outcomes of T cell behavior, we

anticipate that the ultra-potent Delta^{MAX} ligand will be a powerful tool for achieving ideal levels of Notch activation for T cell-related applications.

ACKNOWLEDGMENTS

We would like to thank Dr. Eric Lau, Dr. Gregory Watson and Daniel Lester for their helpful assistance in generating DLL4 stable cell lines. We also thank Dr. Timothy Tran from Moffitt Chemical Biology Core for helping with DSF studies, and Dr. Qianqian Ming for helpful suggestions. D.G. and V.L. were supported by R35GM133482 and an award from the Rita Allen Foundation. S.C.B. is supported by R35CA220340. P.C.R. and S.D. were supported by R01CA184185, R01CA233512; R01CA262121; P01CA250984 Project #4; and P30CA076292; and Florida Department of Health grant #20B04. Support for shared resources was provided by the Moffitt Cancer Center Support Grant NIH P30CA076292.

AUTHOR CONTRIBUTION

V.C.L. and D.G.P. wrote the manuscript. V.C.L., D.G.P, D.A., and P.C.R. designed the experiments. D.G.P. performed the protein purifications, yeast display selections, binding studies, and signaling assays. S.D. performed and designed the T cell experiments with assistance from P.C.R. E.M. contributed to library design and cloning. D.A. performed the detection of Notch activation assays on U2OS and MCF-7 cells by Western blot. E.D.E. and S.C.B. provided U2OS reporter cells and assisted with luciferase experimental procedures. S.C.B., P.C.R., and V.C.L. edited and reviewed the manuscript. V.C.L. supervised and conceived the project.

CONFLICT OF INTEREST

V.C.L., P.C.R., and D.G.P., have filed provisional patents describing the engineering and applications of Delta^{MAX} (application numbers PCT/US2020/041765 and PCT/US2020/030977). V.C.L. is a consultant on an unrelated project for Cellestia Biotech. S.C.B. is on the SAB and receives funding from ERASCA, Inc. for an unrelated project, and is a consultant on unrelated projects for Scorpion Therapeutics, Odyssey Therapeutics, Ayala Pharmaceuticals, MPM Capital, and Droia Ventures.

REFERENCES

1. Sprinzak, D. & Blacklow, S. C. Biophysics of Notch Signaling. *Annu. Rev. Biophys.* **50**, 157–189 (2021).
2. Kopan, R. & Ilagan, Ma. X. G. The Canonical Notch Signaling Pathway: Unfolding the Activation Mechanism. *Cell* **137**, 216–233 (2009).
3. Lovendahl, K. N., Blacklow, S. C. & Gordon, W. R. The Molecular Mechanism of Notch Activation. in *Molecular Mechanisms of Notch Signaling* (eds. Borggrefe, T. & Giaimo, B. D.) vol. 1066 47–58 (Springer International Publishing, 2018).
4. Cordle, J. *et al.* A conserved face of the Jagged/Serrate DSL domain is involved in Notch trans-activation and cis-inhibition. *Nature Structural & Molecular Biology* **15**, 849–857 (2008).
5. Gordon, W. R. *et al.* Mechanical Allostery: Evidence for a Force Requirement in the Proteolytic Activation of Notch. *Developmental Cell* **33**, 729–736 (2015).
6. Gordon, W. R. *et al.* Structural basis for autoinhibition of Notch. *Nat Struct Mol Biol* **14**, 295–300 (2007).
7. Parks, A. L., Klueg, K. M., Stout, J. R. & Muskavitch, M. A. Ligand endocytosis drives receptor dissociation and activation in the Notch pathway. *Development* **127**, 1373–1385 (2000).
8. Seib, E. & Klein, T. The role of ligand endocytosis in notch signalling. *Biol. Cell* **113**, 401–418 (2021).
9. Mumm, J. S. *et al.* A Ligand-Induced Extracellular Cleavage Regulates γ-Secretase-like Proteolytic Activation of Notch1. *Molecular Cell* **5**, 197–206 (2000).
10. De Strooper, B. *et al.* A presenilin-1-dependent γ-secretase-like protease mediates release of Notch intracellular domain. *Nature* **398**, 518–522 (1999).
11. Wu, L. *et al.* MAML1, a human homologue of Drosophila Mastermind, is a transcriptional co-activator for NOTCH receptors. *Nat Genet* **26**, 484–489 (2000).
12. Yamamoto, S. *et al.* A Mutation in EGF Repeat-8 of Notch Discriminates Between Serrate/Jagged and Delta Family Ligands. *Science* **338**, 1229–1232 (2012).
13. Andrawes, M. B. *et al.* Intrinsic selectivity of Notch 1 for Delta-like 4 over Delta-like 1. *J. Biol. Chem.* **288**, 25477–25489 (2013).

462 14. Luca, V. C. *et al.* Structural basis for Notch1 engagement of Delta-like 4. *Science* **347**, 847–
463 853 (2015).
464 15. Luca, V. C. *et al.* Notch-Jagged complex structure implicates a catch bond in tuning ligand
465 sensitivity. *Science* eaaf9739 (2017) doi:10.1126/science.aaf9739.
466 16. Tveriakhina, L. *et al.* The ectodomains determine ligand function in vivo and selectivity of
467 DLL1 and DLL4 toward NOTCH1 and NOTCH2 in vitro. *Elife* **7**, e40045 (2018).
468 17. Hicks, C. *et al.* A secreted Delta1-Fc fusion protein functions both as an activator and
469 inhibitor of Notch1 signaling. *J. Neurosci. Res.* **68**, 655–667 (2002).
470 18. Biktasova, A. K. *et al.* Multivalent Forms of the Notch Ligand DLL-1 Enhance Antitumor T-
471 cell Immunity in Lung Cancer and Improve Efficacy of EGFR-Targeted Therapy. *Cancer*
472 *Res* **75**, 4728–4741 (2015).
473 19. Nandagopal, N. *et al.* Dynamic Ligand Discrimination in the Notch Signaling Pathway. *Cell*
474 **172**, 869-880.e19 (2018).
475 20. Benedito, R. *et al.* The notch ligands Dll4 and Jagged1 have opposing effects on
476 angiogenesis. *Cell* **137**, 1124–1135 (2009).
477 21. Van de Walle, I. *et al.* Specific Notch receptor–ligand interactions control human TCR-αβ/γδ
478 development by inducing differential Notch signal strength. *Journal of Experimental*
479 *Medicine* **210**, 683–697 (2013).
480 22. Nowell, C. S. & Radtke, F. Notch as a tumour suppressor. *Nature Reviews Cancer* **17**, 145–
481 159 (2017).
482 23. Ran, Y. *et al.* γ-Secretase inhibitors in cancer clinical trials are pharmacologically and
483 functionally distinct. *EMBO Mol Med* **9**, 950–966 (2017).
484 24. Goruganthu, M. U. L., Shanker, A., Dikov, M. M. & Carbone, D. P. Specific Targeting of
485 Notch Ligand-Receptor Interactions to Modulate Immune Responses: A Review of Clinical
486 and Preclinical Findings. *Front. Immunol.* **11**, 1958 (2020).
487 25. Espinoza, I. & Miele, L. Notch inhibitors for cancer treatment. *Pharmacology &*
488 *Therapeutics* **139**, 95–110 (2013).
489 26. Tiyanont, K., Wales, T. E., Siebel, C. W., Engen, J. R. & Blacklow, S. C. Insights into
490 Notch3 Activation and Inhibition Mediated by Antibodies Directed against Its Negative
491 Regulatory Region. *Journal of Molecular Biology* **425**, 3192–3204 (2013).

492 27. Xu, X. *et al.* Insights into Autoregulation of Notch3 from Structural and Functional Studies
493 of Its Negative Regulatory Region. *Structure* **23**, 1227–1235 (2015).
494 28. Güner, G. & Lichtenthaler, S. F. The substrate repertoire of γ-secretase/presenilin. *Seminars*
495 *in Cell & Developmental Biology* **105**, 27–42 (2020).
496 29. Komatsu, H. *et al.* OSM-11 Facilitates LIN-12 Notch Signaling during Caenorhabditis
497 elegans Vulval Development. *PLoS Biol* **6**, e196 (2008).
498 30. Liu, L., Wada, H., Matsubara, N., Hozumi, K. & Itoh, M. Identification of Domains for
499 Efficient Notch Signaling Activity in Immobilized Notch Ligand Proteins: CRITICAL
500 DOMAINS OF IMMOBILIZED LIGANDS FOR NOTCH S IGNALING. *J. Cell. Biochem.*
501 **118**, 785–796 (2017).
502 31. Sprinzak, D. *et al.* Cis-interactions between Notch and Delta generate mutually exclusive
503 signalling states. *Nature* **465**, 86–90 (2010).
504 32. Malecki, M. J. *et al.* Leukemia-Associated Mutations within the NOTCH1
505 Heterodimerization Domain Fall into at Least Two Distinct Mechanistic Classes. *Mol Cell*
506 *Biol* **26**, 4642–4651 (2006).
507 33. James, A. C. *et al.* Notch4 reveals a novel mechanism regulating Notch signal transduction.
508 *Biochimica et Biophysica Acta (BBA) - Molecular Cell Research* **1843**, 1272–1284 (2014).
509 34. Trotman-Grant, A. C. *et al.* DL4-μbeads induce T cell lineage differentiation from stem cells
510 in a stromal cell-free system. *Nat Commun* **12**, 5023 (2021).
511 35. Mohtashami, M. *et al.* Direct Comparison of Dll1- and Dll4-Mediated Notch Activation
512 Levels Shows Differential Lymphomyeloid Lineage Commitment Outcomes. *The Journal of*
513 *Immunology* **185**, 867–876 (2010).
514 36. Safaee, H. *et al.* Tethered Jagged-1 Synergizes with Culture Substrate Stiffness to Modulate
515 Notch-Induced Myogenic Progenitor Differentiation. *Cel. Mol. Bioeng.* **10**, 501–513 (2017).
516 37. Bheeshmachar, G. *et al.* Evidence for a Role for Notch Signaling in the Cytokine-Dependent
517 Survival of Activated T Cells. *J Immunol* **177**, 5041–5050 (2006).
518 38. Cho, O. H. *et al.* Notch regulates cytolytic effector function in CD8+ T cells. *J Immunol* **182**,
519 3380–3389 (2009).
520 39. Palaga, T., Miele, L., Golde, T. E. & Osborne, B. A. TCR-Mediated Notch Signaling
521 Regulates Proliferation and IFN-γ Production in Peripheral T Cells. *J Immunol* **171**, 3019–
522 3024 (2003).

523 40. Adler, S. H. *et al.* Notch Signaling Augments T Cell Responsiveness by Enhancing CD25
524 Expression. *J Immunol* **171**, 2896–2903 (2003).
525 41. Joshi, I. *et al.* Notch signaling mediates G1/S cell-cycle progression in T cells via cyclin D3
526 and its dependent kinases. *Blood* **113**, 1689–1698 (2009).
527 42. Thomas, A. K., Maus, M. V., Shalaby, W. S., June, C. H. & Riley, J. L. A Cell-Based
528 Artificial Antigen-Presenting Cell Coated with Anti-CD3 and CD28 Antibodies Enables
529 Rapid Expansion and Long-Term Growth of CD4 T Lymphocytes. *Clinical Immunology*
530 **105**, 259–272 (2002).
531 43. Eagar, T. N. *et al.* Notch 1 Signaling Regulates Peripheral T Cell Activation. *Immunity* **20**,
532 407–415 (2004).
533 44. Backer, R. A. *et al.* A central role for Notch in effector CD8(+) T cell differentiation. *Nat*
534 *Immunol* **15**, 1143–1151 (2014).
535 45. Sierra, R. A. *et al.* Rescue of Notch-1 Signaling in Antigen-Specific $CD8^{+}$ T Cells
536 Overcomes Tumor-Induced T-cell Suppression and Enhances Immunotherapy in Cancer.
537 *Cancer Immunol Res* **2**, 800–811 (2014).
538 46. Delaney, C., Varnum-Finney, B., Aoyama, K., Brashem-Stein, C. & Bernstein, I. D. Dose-
539 dependent effects of the Notch ligand Delta1 on ex vivo differentiation and in vivo marrow
540 repopulating ability of cord blood cells. *Blood* **106**, 2693–2699 (2005).
541
542
543
544
545
546
547
548
549
550
551
552
553

554 **FIGURES**

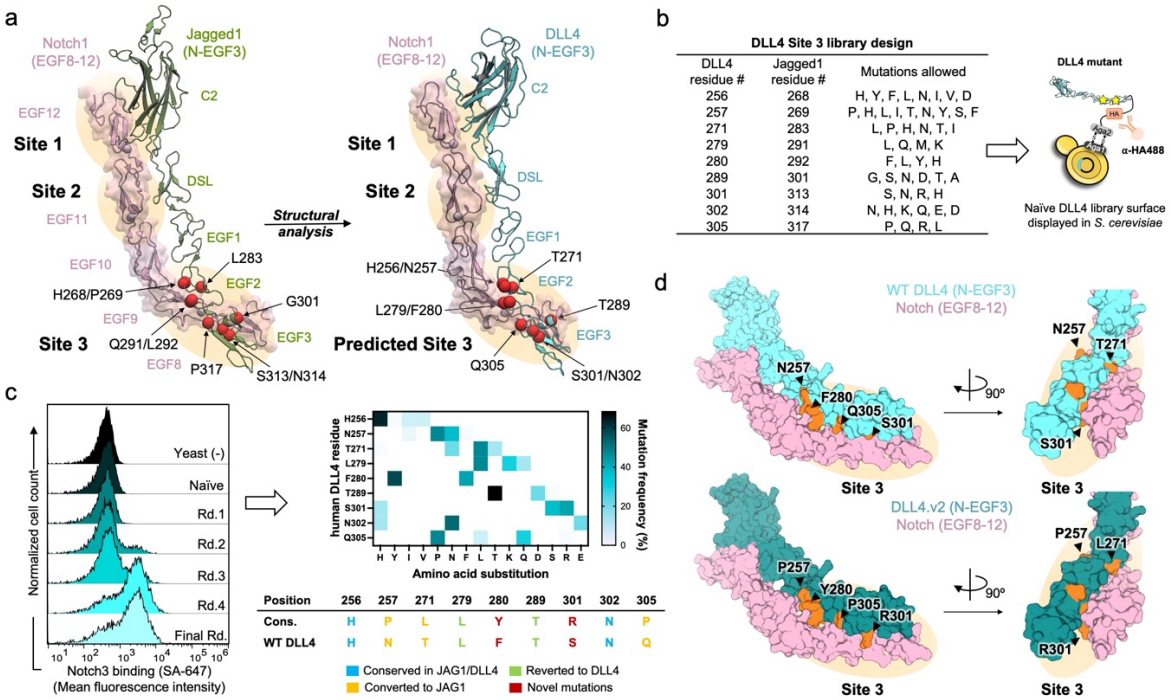

555

556 **Fig 1. Yeast display selection of affinity-enhancing mutations in DLL4.** (**A**) Cartoon schematic
557 of the design strategy for the DLL4 Site 3 mutant library. Red spheres depict mutated interface
558 residues. (**B**) Table depicting DLL4 interface residue positions and the mutations allowed at each
559 position and schematic of DLL4 yeast display construct. Yellow stars indicate mutations. (**C**) Flow
560 cytometry histogram plots of yeast stained with fluorescently-labeled Notch3 protein following
561 each round of selection (left), and a table indicating the frequency of mutations and consensus
562 DLL4 mutant sequence (right). (**D**) Structural models highlighting the mutated residues in
563 DLL4.v2. WT residues in DLL4 and mutated residues in DLL4.v2 are colored orange and shown
564 in surface representation. DLL4 models were based on DLL4:Notch1 (PDB ID: 4XL1, for C2-
565 DSL-EGF1 domains) and Jagged1:Notch1 (PDB ID:5UK5, for EGF1-EGF3) structures.

566

567

568

569

570

571

572

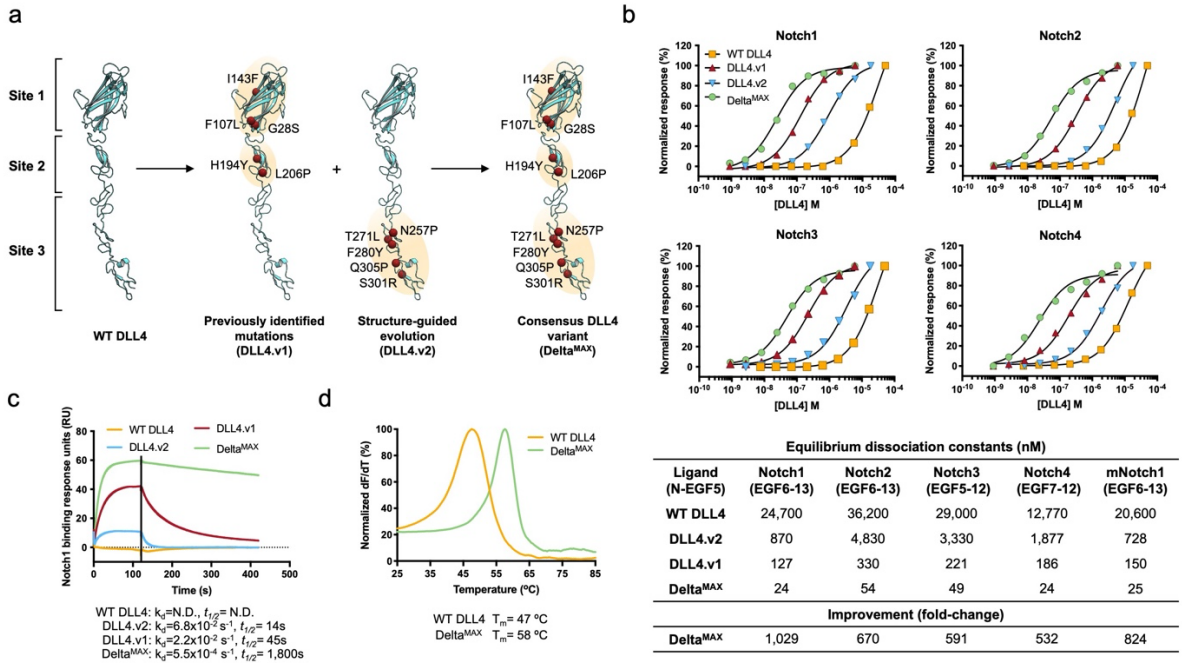

Equilibrium dissociation constants (nM)

Ligand (N-EGF5)	Notch1 (EGF6-13)	Notch2 (EGF6-13)	Notch3 (EGF5-12)	Notch4 (EGF7-12)	mNotch1 (EGF6-13)
WT DLL4	24,700	36,200	29,000	12,770	20,600
DLL4.v2	870	4,830	3,330	1,877	728
DLL4.v1	127	330	221	186	150
Delta^{MAX}	24	54	49	24	25
Improvement (fold-change)					
Delta^{MAX}	1,029	670	591	532	824

Fig 2. Biophysical characterization of Delta^{MAX} variant. (**A**) Schematic depicting the generation of DLL4^{MAX} through engraftment of DLL4.v1 and DLL4.v2 mutations. Red spheres indicate affinity-enhancing mutations. (**B**) SPR binding isotherms measuring DLL4 variant interactions with the ligand binding domains of Notch1-4. The table shows the K_D determined for each interaction and the fold-enhancement of DLL4^{MAX} affinity relative to WT DLL4. (**C**) Representative SPR sensograms depicting the binding of 200 nM concentrations of WT DLL4, DLL4.v1, DLL4.v2, and DLL4^{MAX} to Notch1 EGF6-13. (**D**) DSF was used to determine the T_m of WT DLL4 and Delta^{MAX}.

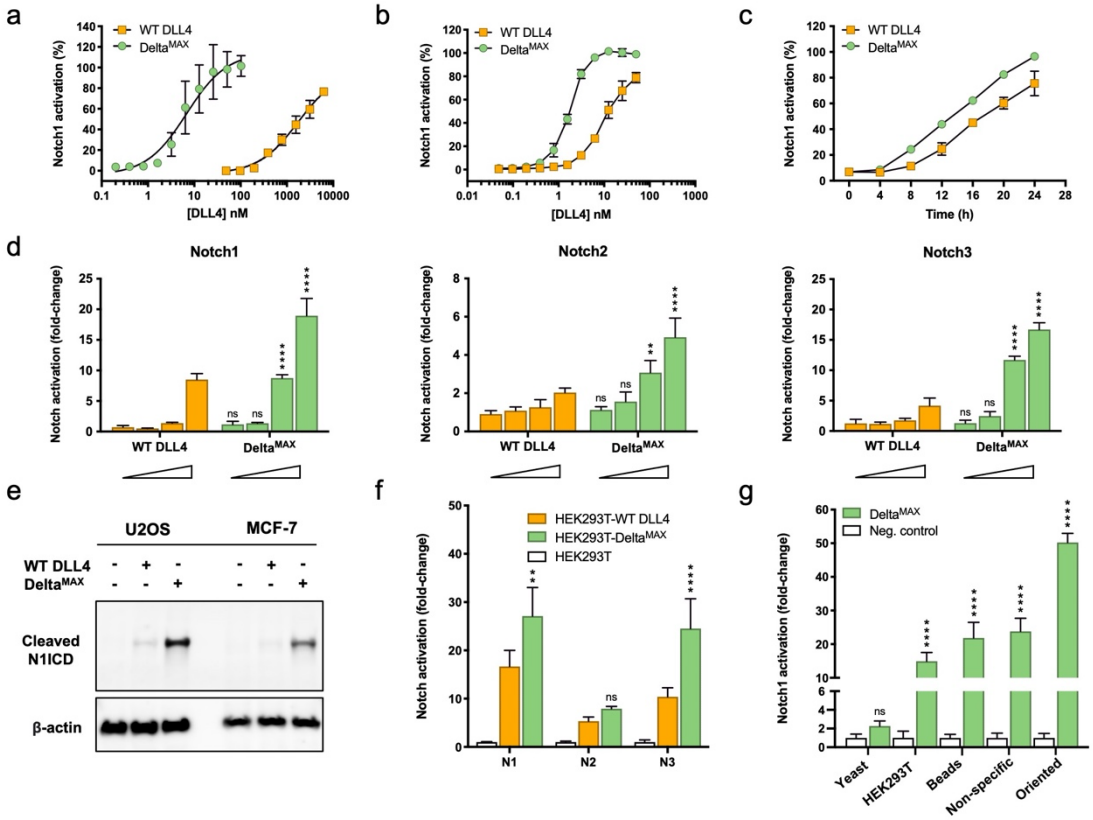

Fig 3. Delta^{MAX} is more potent Notch agonist than WT DLL4. (**A**) Dose-titration assay comparing the Notch1 reporter activity stimulated by WT DLL4 and Delta^{MAX} proteins that were non-specifically adsorbed to tissue culture plates. (**B**) Dose-titration assay comparing the Notch1 reporter activity stimulated by WT DLL4 and Delta^{MAX} proteins. DLL4 ligands were C-termini biotinylated and coupled to streptavidin-coated plates. (**C**) Time-course experiment comparing Notch1 reporter activity stimulated by WT DLL4 or Delta^{MAX} immobilized at 50 nM. (**D**) A luciferase reporter assay was used to measure Notch1, Notch2, or Notch3 activation by WT DLL4 and DLL4^{MAX}. Protein concentrations were a 10-fold serial dilution from 50 nM to 0.05 nM. (**E**) Detection of endogenous cleaved Notch intracellular domain (N1ICD) in U2OS and MCF-7 cell lines by Western blot. Cells were Notch activated with 50 nM of WT DLL4 and Delta^{MAX} immobilized in streptavidin plates. (**F**) Co-culture assay comparing Notch1 activation by Delta^{MAX} and WT DLL4. Notch1 reporter cells and ligand-expressing cells were cultured at a 1:1 ratio. (**G**) Notch1 luciferase reporter cells were stimulated with Delta^{MAX} protein in different formats. Yeast expressing Delta^{MAX} were co-cultured in 10:1 ratio with reporter cells; HEK293T cells stably expressing Delta^{MAX} were co-cultured in 1:1 ratio; Delta^{MAX}-coated streptavidin beads were mixed in 20:1 ratio; 100 nM Delta^{MAX} was non-specifically adsorbed to surfaces prior to addition of

609 reporter cells; 10 nM C-terminally biotinylated Delta^{MAX} was immobilized on streptavidin-coated
610 plates. Notch activation was normalized to the corresponding controls. Delta^{MAX} statistics are
611 referred to WT DLL4. *P<0.05, **P<0.01, ****P<0.0001, ns: not significant (Two-way
612 ANOVA).
613
614
615
616
617
618
619
620
621
622
623
624
625
626
627
628
629
630
631
632
633
634
635

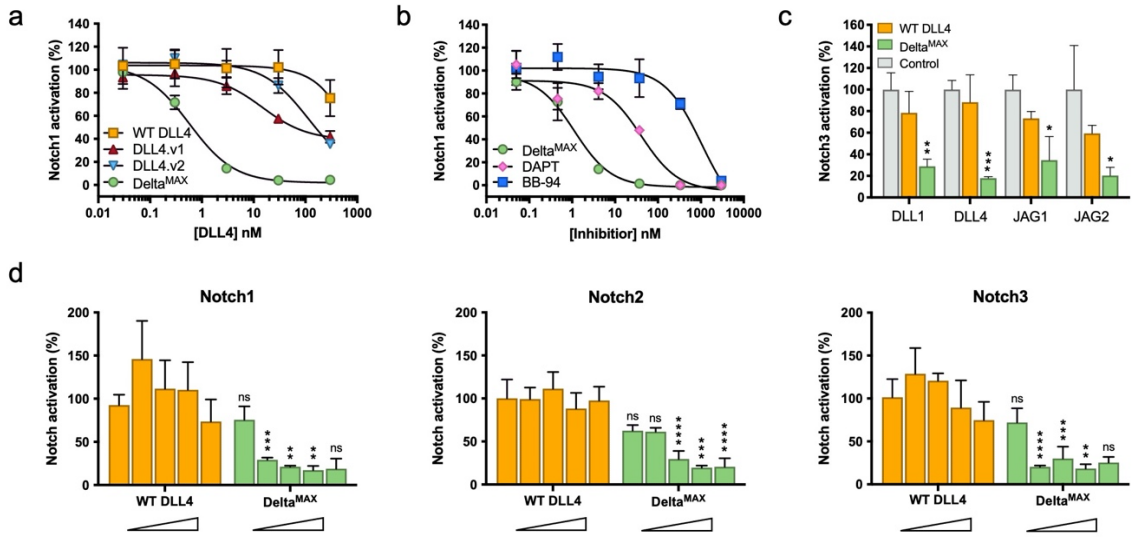

Fig 4. Delta^{MAX} is a pan-Notch inhibitor. (**A**) Dose-titration assay measuring the inhibition of Notch1 reporter activity by soluble DLL4 variants. Notch1 signaling was activated by culturing cells on streptavidin plates coated with 50 nM WT DLL4. (**B**) Dose-titration assay comparing the inhibition potency of DAPT, BB-94, and soluble Delta^{MAX}. Notch1 signaling was activated by culturing cells on streptavidin plates coated with 50 nM WT DLL4. (**C**) Soluble WT DLL4 and Delta^{MAX} at 3 μM were tested for their ability to inhibit Notch1 activation by 293T cells overexpressing DLL4, DLL1, JAG1, or JAG2. (**D**) Dose-titration assay comparing the ability of WT DLL4 and Delta^{MAX} to inhibit activation of Notch1-3 by WT DLL4. 10-fold serial dilutions starting at 3,000 nM of soluble DLL4 or Delta^{MAX} were added to Notch1, Notch2, and Notch3 luciferase reporter cells. Notch signaling was activated by culturing cells on streptavidin plates coated with 50 nM WT DLL4. *P<0.05, **P<0.01, ***P<0.001, ****P<0.0001, ns: not significant (Two-way ANOVA).

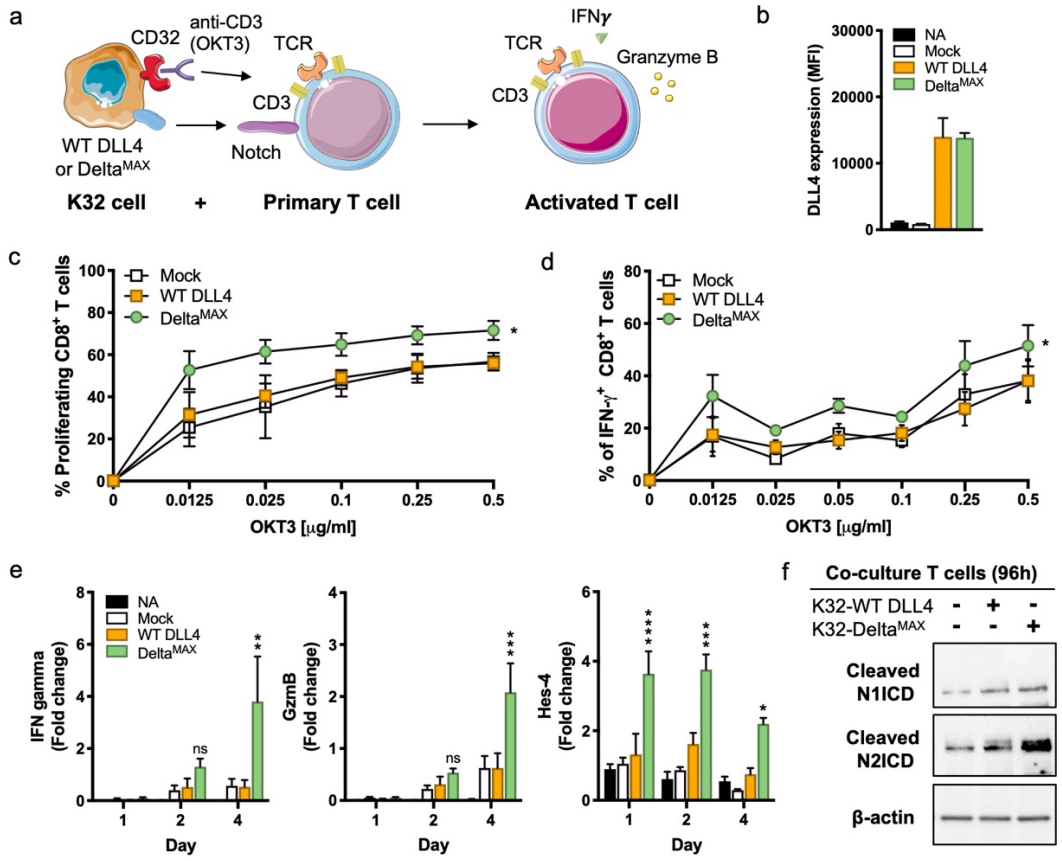

Fig 5. Translational strategy to transiently boost Notch signaling in human CD8$^+$ T cells. (**A**) Human PBMCs CD8$^+$ T cells were co-cultured with K32 artificial antigen-presenting cells (aAPCs) engineered to express WT DLL4 or Delta^{MAX} for simultaneous Notch and TCR stimulation. (**B**) aAPCs were assayed for expression of WT DLL4 or Delta^{MAX} using flow cytometry. K32 cells were loaded with OKT3 antibody using a gradient of concentrations starting at 0.0125 μg/ml, and then co-cultured with CD8$^+$ T cells in ratio 10:1. After 96h, CD8$^+$ T cells were analyzed for proliferation (**C**) and IFNγ secretion (**D**). **(E)** T cells were stimulated for 24, 48, and 96h to quantify mRNA levels of intracellular activation markers by real-time PCR, including IFNγ, Granzyme B and Hes-4. (**F**) K32 cells expressing WT DLL4 or Delta^{MAX} were co-culture with human CD8$^+$ T cells (ratio 1:10) for detection of Notch activation by Western blot. Co-cultured CD8$^+$ T cells were positively sorted by MACS column after cultivation with K32 cells, and nuclear extracts were harvested after 96 hours. Cleavage of Notch1 and Notch2 were examined by Western blot with specific antibodies. β-actin was used for loading control. Western blot images are representative results of 3 biological repeats. NA: non-activated T cells. Statistics for Delta^{MAX}

672 are referred to WT DLL4. *P<0.01, **P<0.001, ***P<0.001, ***P<0.0001, ns: not significant
673 difference (Two-way ANOVA). T cell proliferation and IFNγ secretion data were analyzed by
674 unpaired t tests.
675

Extended Data Material

An affinity-matured DLL4 ligand for broad-spectrum activation and inhibition of Notch signaling

David Gonzalez-Perez[1], Satyajit Das[2], Elliot Medina[1], Daniel Antfolk[1], Emily D. Egan[3], Stephen C. Blacklow[3], Paulo C. Rodriguez[2], and Vincent C. Luca[1*].

[1] Department of Drug Discovery, Moffitt Cancer Center, Tampa, FL 33602, USA

[2] Department of Immunology, Moffitt Cancer Center, Tampa, FL 33612, USA

[3] Department of Biological Chemistry and Molecular Pharmacology, Harvard Medical School, Boston, Massachusetts 02115; Department of Cancer Biology, Dana Farber Cancer Institute, Boston, Massachusetts 02115, USA

[*] Corresponding author: vince.luca@moffitt.org

MATERIAL AND METHODS

Reagents, media, and cell lines

Mammalian cells were cultured at 37°C, with a humidified atmosphere of 5% CO_2, washed with Dulbecco's Phosphate Saline Buffer (DPBS, Corning), and detached with Trypsin-EDTA 0.25% (Gibco) for cell sub-culturing or cell-based assays. Notch reporter cell lines CHO-K1 hNotch1-Gal4 were a gift from Dr. Michael Elowitz (California Institute of Technology)[1]. HEK293T, U2OS and MCF-7 cells were cultured in high-glucose Dulbecco Eagle's Minimal Essential Medium (DMEM, Cytiva) supplemented with 10% Fetal Bovine Serum (FBS, peak serum) and 2% penicillin/streptomycin (Gibco). The MCF-7 breast cancer cell line was a gift from Dr. Eric Lau (Moffitt Cancer Center). Hygromycin 100 µg/ml was added to U2OS reporter[2] cell cultures to maintain homogeneous populations of Notch-expressing cells. CHO-K1 hNotch1-Gal4 cells were cultured in Minimum Essential Medium Eagle-alpha modification (α-MEM, Cytiva) supplemented with 10% Fetal Bovine Serum (FBS, peak serum), 2% penicillin/streptomycin (Gibco), 400 µg/mL of Zeocin (Alfa aesar) and 600 µg/mL of Geneticin (Gibco). K32 cells (K562 cell line expressing CD32) were a gift from Dr. Jose Conejo-Garcia (Moffitt Cancer Center), and human $CD8^+$ T cells were PBMCs (collected from LifeSouth Blood Bank, Gainesville, FL). Cells used for T cell experiments were cultured at 37°C, and 5% CO_2, in RPMI-1640 (Gibco) supplemented with 2 mM L-glutamine, 10 mM HEPES, 150 U/mL streptomycin, 200 U/mL Penicillin, 20 mM β-mercaptoethanol and 10% heat-inactivated FBS (GeminiBio). All cell lines were tested negative for mycoplasma (ATCC), and stable cell lines were validated by sequencing (Genewiz) after genomic DNA extraction (Invitrogen). Antibodies used in this study were: anti-hNotch1 PE (Biolegend), anti-hNotch2 AF647 (Biolegend), anti-hNotch3 PE (Biolegend), anti-hDLL4 PE (Biolegend), anti-hDLL1 PE (Biolegend), anti-hJagged1 AF647 (Biolegend), anti-hJagged2 PE (Biolegend), and anti-HA tag AF488 (Cell Signaling Technologies), anti-hCD8a Bv785 (Biolegend), anti-hIFNγ APC (Biolegend), goat anti-mouse IgG (secondary antibody, KPL), goat anti-rabbit IgG (secondary antibody, Vector laboratories), anti-cleaved Notch1 (Val1744, Cell Signaling Technology), anti-Notch2 (D76A6, Cell Signaling Technologies), anti-β-Actin (Cell Signaling Technology and Sigma).

63 **Protein expression and purification**

64 The minimum binding region of Delta-Like 4 (DLL4) fragments (N-EGF5) were cloned into the
65 pAcGp67A vector containing an N-terminal gp67 signal peptide and C-terminal 8xHis-tag. Non-
66 biotinylated proteins were human wild-type DLL4 (N-EGF5, residues 27-400), DLL4.v1 (N-
67 EGF5), DLL4.v2 (N-EGF5), and $DLL4^{MAX}$ (N-EGF5). Notch biotinylated fragments were cloned
68 into pAcGp67A with a N-terminal gp67 signal peptide, a C-terminal 3C protease site followed by
69 biotin-acceptor peptide tag (BAP-tag: GLNDIFEAQKIEWHE), and 6xHis-tag. In contrast, DLL4
70 biotinylated proteins contained BAP and His-tags, but lacked 3C site. Biotinylated proteins were
71 human Notch1 (EGF8-12, residues 295-488), hNotch1 (EGF6-13, residues 237-549), hNotch2
72 (EGF6-13, residues 221-530), hNotch3 (EGF5-12, residues 197-505), hNotch4 (EGF7-12,
73 residues 276-511), mouse Notch1 (EGF6-13, residues 221-526), WT DLL4 (N-EGF5, residues
74 27-400), and $DLL4^{MAX}$ (N-EGF5, residues 27-400). All baculovirus-based constructs in this work
75 were expressed for 48 hours by infecting HiFive *Trichoplusia ni* insect cell cultures (Expression
76 Systems) at a density of $2x10^6$ cells/mL with infective baculovirus particles. Culture supernatants
77 were harvested, and proteins purified by IMAC. Ni-NTA agarose resin (Qiagen) was washed with
78 HEPES Buffered Saline (HBS: 20 mM HEPES pH 7.4, 150 mM sodium chloride; Buffer A)
79 supplemented with 25 mM imidazole (plus 1 mM calcium chloride for Notch preps; Buffer A+C)
80 and eluted with Buffer A (or Buffer A+C for Notch samples) containing 250 mM imidazole.
81 Polishing was performed using a Superdex 200 Increase 10/300 GL column (GE) equilibrated in
82 Buffer A for DLL4 proteins, or Superdex 75 Increase 10/300 GL column (GE) equilibrated in
83 Buffer A+C for Notch proteins. Biotinylated proteins were site-specifically modified *in vitro* at
84 their C-terminal BAP-tag, using BirA ligase (in-house prepared) and polished as described above.
85 Protein purity and integrity were analyzed by SDS-PAGE using TGX 12% Pre-cast gels (Bio-
86 Rad). All proteins were flash frozen in liquid nitrogen and stored at -80°C for later use.

87

88 **Affinity maturation of human DLL4 by directed evolution**

89 *Starting point of evolution and structure-guided library creation*

90 Wild-type human Delta-like 4 (N-EGF3, residues 27-322) was cloned into a modified version of
91 pCT302 an N-terminal fusion to an HA-epitope (YPYDVPDYA), c-Myc epitope
92 (EQKLISEEDL), and Aga2. A third binding site for DLL4:Notch interaction was designed on the
93 basis of the binding interface found in the crystal structure of rJagged1(N-EGF3):rNotch1(EGF8-

12) complex[3]. The complex was analyzed with different computational tools (PDBePISA (EMBL-EBI), Consurf server (Biosof), and PyMOL (Schrödinger)). Nine interface residues were selected to create a structure-guided directed evolution library. Jagged1 homolog residues were identified in DLL4 and targeted for mutagenesis. The mutant library was generated using assembly PCR with the ten overlapping oligonucleotides below:

Lib1F:
CAGCCTATCTGTCTTTCGGGCTGTCATGAACAGAATGGCTACTGCAGCAAGC

Lib2R:
GCCAGCCTGGGCGGCAGAGGCACTCGGCCGGCTTGCTGCAGTAGCCATTC

Lib3F:
TCTGCCGCCCAGGCTGGCAGGGCCGGCTGTGTAACGAATGCATCCCC

Lib4R:
CCAGGGAGTGCTGCAGGTGCCGTGGCGACAGCC**ADDAWN**GGGGATGCATTCGTTACACAG

Lib5F:
CACCTGCAGCACTCCCTGGCAATGT**MHT**TGTGATGAGGGCTGGGGAG,

Lib6R:
GCAGTAGTTGAGATCTTGGTCACA**AWRCWK**GCCTCCCCAGCCCTCATCACA

Lib7F:
GTGACCAAGATCTCAACTACTGC**RVT**CACCACTCCCCATGCAAGAATGGGGCAACGTGC

Lib8R:
GGCGACAGGTGCAGGTGTAGCTTCG**CNG**CCCACT**WTBAYK**GCACGTTGCCCCATTCTTG

Lib9F:
CTACACCTGCACCTGTCGCCCGGGCTACACTGGTGTGGACTGTGAGGGATCCTACCCATAC

Lib10R:
AGATAAGCTTTTGTTCTCCACCAGCGTAATCTGGAACATCGTATGGGTAGGATCCCTCAC).

125 The primers contained specific degenerate codons (bold underlined) and 20bp overhangs
126 (Eurofins) to promote annealing in the PCR reaction. External primers were added to introduce a
127 40-50 bp recombination area between the mutant library region (EGF1-EGF3) and DLL4-pYAL
128 linearized vector. The mutant library was *in vivo* reassembled into yeast by electroporation (BTX
129 electroporator) with 10 µg of linearized DLL4-pYAL vector and 50 µg of the mutagenic library
130 (ratio 1:5 vector:library). Yeast transformants were recovered in SDCAA and DLL4 surface
131 displayed on *S. cerevisiae* EBY100 yeast as reported previously[3,4]. The theoretical library diversity
132 was 4x10E6, and we obtained an estimated library size of 8x10E6 variants (2-fold theoretical
133 diversity).
134
135 **Yeast display selections**
136 Before starting each selection round, induced yeast cultures were pelleted in logarithmic phase,
137 stained with anti-HA antibody conjugated to AF488 (Cell Signaling Technologies), and expression
138 of DLL4 on yeast surface analyzed by flow cytometry (BD Accuri C6 Plus). Selection rounds were
139 performed in two phases: (1) a negative selection to remove non-specific binders targeting
140 streptavidin and/or Alexa Fluor 647, and (2) a positive selection to rescue high-affinity variants
141 specific for Notch. Negative selection was performed by combining 100 nM of streptavidin
142 conjugated to Alexa Fluor 647 (SA647) and 250 µL anti-Alexa Fluor 647 magnetic beads
143 (Miltenyi) on ice for 10 min. Next, the yeast library was washed once in selection buffer (HBS: 20
144 mM HEPES pH 7.4, 150 mM sodium chloride, 1 mM calcium chloride, 0.1% Bovine Serum
145 Albumin (BSA) and 10 mM maltose), and magnetic beads SA647-coated were added. The tube
146 was wrapped in foil and incubated at 4°C for 30 min. Following this step, the yeast was washed
147 twice with selection buffer, resuspended, and flowed over a Magnetic-Activated cell sorting
148 (MACS) LS separation column (Miltenyi) pre-equilibrated in selection buffer. The flowthrough
149 was rescued, and positive selections were performed. For round zero (Naïve library), 8x10E7 cells
150 (10x library diversity) were used for selection against biotinylated Notch1 (EGF8-12) and Notch3
151 (EGF5-13), independently. Tetramers were pre-made on ice for 10 min by mixing 450 nM of
152 biotinylated Notch1 (EGF8-12) or Notch3 (EGF5-12) with 100 nM of SA-647 (ratio 4.5:1). Next,
153 100 nM tetramers were added to 500 µL of negatively selected yeast in selection buffer and
154 incubated for 2 hours at 4°C. Yeast library stained with Notch tetramers was washed twice with
155 500 µL of selection buffer, and further incubated with 50 µL of anti-AF647 magnetic beads for 30

156 min at 4°C. After incubation, the yeast was washed twice with 500 µL of selection buffer and high-
157 affinity binders isolated by MACS columns. The isolated yeast cells were pelleted, recovered in 3
158 mL of SDCAA for 48 hours and induced in SGCAA for next round. For round 1, the same
159 conditions were repeated like in round zero using Notch1 (EGF8-12) and Notch3 (EGF5-12) 100
160 nM tetramers for positive selections. Isolated populations were rescued in 3 mL SDCAA after
161 MACS sorting and induced in SGCAA. For round 2, 5x10E7 yeast cells were resuspended in 500
162 µL of selection buffer in the presence of 2 µM monomer of Notch1 (EGF8-12) and Notch3 (EGF5-
163 12), independently. Tubes were wrapped in foil and incubated for 2 hours at 4°C. Yeast samples
164 binding Notch were washed twice with 500 µL of selection buffer, and incubated in 500 µL of
165 selection buffer supplemented with 100 nM of SA-647 for 30 min at 4°C. DLL4 high-affinity
166 binders were isolated by MACS following the same approach described for rounds 1 and 2. High-
167 affinity binders for Notch1 and Notch3 were rescued in 3 mL of SDCAA for 48 hours and induced
168 in SGCAA. For round 3, high-affinity populations were isolated by Fluorescent-Activated Cell
169 Sorting (FACS, Sony Sorter SH800S). Only Notch3 (EGF5-12) was used since yeast-staining tests
170 showed better population enrichment compared with Notch1 (EGF8-12). 1x10E8 yeast cells were
171 resuspended into 500 µL of selection buffer with pre-made 100 nM tetramers of Notch3 (5-12)
172 and anti-HA488 antibody (double staining). The tube was wrapped in foil and incubated for 2
173 hours at 4°C. Stained yeast was washed two times with 500 µL of selection buffer and analyzed
174 by FACS. From the double-positive population (FIT-C+, APC+) showing expression of DLL4
175 (anti-HA488, FIT-C signal) and binding to Notch (SA-647, APC signal), a sorting gate was set at
176 1.8% of the maximum signal detected for APC channel and Notch binders isolated (Extended Data
177 Fig 1b). The sorted yeast population was washed two times with 5 mL of selection buffer, pelleted,
178 and recovered in SDCAA for 48 hours. Yeast cells were induced again in SGCAA for the last
179 round of selection. For round 4, 5x10E7 cells were incubated with 0.2 µM monomers of Notch3
180 (5-12) for 2 hours at 4°C. Yeast cells were then washed twice with selection buffer, fluorescent-
181 labeled with SA-647 and high-affinity populations isolated by MACS following the protocol
182 described for previous rounds.
183 The isolated yeast populations obtained after round 4 were subjected to colony screen and plasmid
184 recovery by using Zymoprep kit (Zymo Research). The plasmids were transformed into *E. coli*
185 and 30 individual colonies sequenced with pYAL F (5'-AAATGATAACCATCTCGC) and pYAL

186 R (5'-GGGATTTGCTCGCATATAGTTG) primers (Eurofins). Sequencing data analysis was
187 performed using SnapGene software (Insightful Science).
188
189 **Generation of DLL4 variants**
190 We first generated a variant named DLL4.v1 by engrafting five affinity enhancing mutations into
191 human DLL4 scaffold that we previously reported for rat DLL4 affinity maturation (Site 1 + Site
192 2; G28S, F107L, I143F, H194Y, and L206P)[4]. Next, the mutations found in this work to create a
193 third binding site on human DLL4 (Site 3; N257P, T271L, F280Y, S301R, Q305P) were combined
194 with Site 1 + Site 2 mutations into one single DLL4 scaffold, creating an ultrapotent DLL4 protein,
195 named Delta^{MAX} (Site 1 + Site2; G28S, F107L, I143F, H194Y and L206P, and Site 3; N257P,
196 T271L, F280Y, S301R, Q305P).
197
198 **Thermal denaturation experiments by differential scanning fluorometry (DSF)**
199 WT DLL4 and Delta^{MAX} (N-EGF5) were diluted at 5 µM in 20 µL of HBS buffer, and then
200 combined with 10 µM (5x) SYPRO Orange (ThermoFisher Scientific) prepared in 100% DMSO
201 (final DMSO concentration was 0.1%). This mix was equilibrated at room temperature for 30 min.
202 Proteins were analyzed in a 96-well microtiter plate using a StepOnePlus RT-PCR system (Applied
203 Biosystems) applying a continuous heating gradient from 25 to 99ºC with a step of 1% of
204 temperature/min. Data was normalized and represented as the mean of three independent technical
205 replicates. Similar Tm values were obtained for the replica measurements.
206
207 **Determination of equilibrium dissociation constants (K_D) by Surface Plasmon Resonance**
208 **(SPR)**
209 Equilibrium dissociation constants were determined by surface plasmon resonance using a Biacore
210 T200 instrument (GE Healthcare). Approximately 100 resonance units (RU) of biotinylated Notch
211 extracellular fragments (Notch1 (EGF6-13), Notch2 (EGF6-13), Notch3 (EGF5-12), Notch4 (7-
212 12), and mouse Notch1(EGF6-13)) were immobilized on individual flow cells at 5 µl/min using a
213 streptavidin-coated sensor chip (Series S Sensor chip SA, GE Healthcare). Three-fold serial
214 dilutions of recombinant DLL4 proteins (N-EGF5) starting at 50 µM (WT DLL4), 18 µM
215 (DLL4.v2), and 6 µM (DLL4.v1 and Delta^{MAX}) were flowed over the chip at 25°C in SPR buffer
216 (20 mM HEPES pH 7.4, 150 mM NaCl, 1 mM calcium chloride, 0.1% BSA supplemented with

217 0.005% surfactant P20). Association ("on-rate") and dissociation ("off-rate") phases were
218 performed at 10 µl/min for 120 seconds and 300 seconds, respectively. The sensor chip was
219 regenerated after each injection with 30-second washes of 2.25M Magnesium Chloride containing
220 25% Ethylene Glycol at 50 µL/min. Data collection rate was performed at 10Hz, and curves were
221 reference-subtracted from a flow cell containing 100 RU of a negative control non-related protein
222 (biotinylated mouse RNF43 PA domain). The maximum RU for each experiment was normalized
223 to a value of 100% and plotted as a function of concentration using Prism 9 software (GraphPad).
224 Steady-state binding and kinetic curves were fitted using the Biacore T200 evaluation software to
225 a 1:1 Langmuir model to determine the K_D values.
226
227 **Generation of stable cell lines**
228 Ectodomains of WT DLL4 and Delta^{MAX} (N-EGF8, residues 27-518) were cloned into an
229 intermediary vector containing WT DLL4 signal peptide, juxtamembrane, transmembrane, and
230 intracellular domain, fused to C-terminal Myc (EQKLISEEDL) and Flag (DYKDDDDK) tags.
231 This vector was generated after cloning of a synthetic DNA fragment (Eurofins) into pLenti-C-
232 Myc-DDK-IRES-Puro vector (Invitrogen). For stable cell lines expressing DLL1 (residues 1-723),
233 Jagged1 (residues 1-1218), and Jagged2 (residues 1-1238), their CDS was cloned into pLenti-C-
234 Myc-DDK-IRES-Puro vector fused to c-Myc and Flag C-termini tags. HEK-293T mammalian
235 cells were used for lentiviral particle production and transductions (kindly donated by Dr. Eric
236 Lau, Moffitt Cancer Center). Briefly, transfections were carried out with packaging vectors VSV-
237 G and d8.9 (kindly donated by Dr. Eric Lau, Moffitt Cancer Center) in the presence of
238 Polyethyleneimine (PEI) at ratio 4:1 (DNA:PEI). Lentiviral particles were harvested after 48-72
239 hours and used to transduce HEK293T cells using 1 µg/mL polybrene (Millipore). Antibiotic
240 selection was performed using Puromycin at 5 µg/mL (Gibco) for 10-15 days. Puromycin resistant
241 cells expressing WT DLL4 and Delta^{MAX} were detached with trypsin-free dissociation buffer
242 (Gibco), stained in DPBS + 0.5% BSA with anti-hDLL4 PE antibody for 1 hour at 4°C, and then
243 sorted by FACS (Sony sorter SH800S). Sorted cells (mean fluorescence intensity around 1x10E5-
244 3x10E5) were washed with DPBS and recovered in DMEM+10% FBS at 37°C and 5% CO_2 for 2
245 weeks. Expression of WT DLL4 and Delta^{MAX} on HEK293T surface was confirmed by flow
246 cytometry (BD Accuri C6 plus) staining the cell lines with anti-hDLL4 PE in DPBS + 0.5% BSA
247 (Extended Data Fig 7b). DLL1, Jagged1, and Jagged2 cell lines were stained with specific

248 antibodies (anti-hDLL1 PE, anti-hJagged1 AF647, and anti-hJagged2 PE) for 1 hour at 4°C and
249 analyzed by flow cytometry (BD Accuri C6 plus); however, these cell lines did not require further
250 sorting steps (Extended Data Fig. 10).
251
252 K32 cells (K562 cells expressing human CD32) were transduced with lentivirus expressing WT
253 DLL4 or Delta^{MAX} by spin-infection using 8 µg/mL polybrene (Millipore). Seventy-two hours after
254 transduction, cells were analyzed for DLL4 expression and further cultured in RPMI + 10% FBS
255 containing 1 µg/ml of puromycin (Gibco) at 37 ºC and 5% CO_2. DLL4 expression was monitored
256 by flow cytometry (CytoFLEX II, Beckman Coulter) using anti-hDLL4 PE (Biolegend) until the
257 culture reached ~100% of positive population on PE signal.
258
259 **Notch activation assays with ligands non-specifically adsorbed to plates**
260 On day one, 2-fold serial dilutions of non-biotinylated DLL4 recombinant proteins (N-EGF5) were
261 prepared in 100 µL of DPBS and used to coat 96-well plates (Coastar) for 1 hour at 37°C. WT
262 DLL4 started at 50 µM and Delta^{MAX} at 204 nM. Then, the wells were washed three times with
263 200 µL of DPBS to remove unbound proteins. Next, CHO-K1 Notch1-Gal4 cells in culture were
264 detached with trypsin-EDTA 0.25% (Gibco) and manually counted. Appropriate dilutions were
265 prepared in α-MEM media to ensure 30,000 CHO-K1 cells per well in 200 µL. Ligand-coated
266 plates and reporter cell lines were incubated for 24 hours at 37°C and 5% CO_2. On day two, CHO-
267 K1 Notch1-Gal4 cells were washed with 200 µL DPBS, detached with 30 µL of trypsin-EDTA
268 0.25%, and quenched with 200 µL of α-MEM media. Finally, cells were resuspended and H2B-
269 mCitrine signal was measured by flow cytometry (BD Accuri C6 plus). CHO-K1 Notch1-Gal4
270 and ligand-lacking wells were used as a negative control. The measurements represent the mean
271 fluorescent intensity as percentage of Notch activation ± S.D. of three biological replicates. Notch
272 activation was reference-subtracted from a well coated with 0.5% BSA containing CHO-K1 cells.
273 Gating strategies for this experiment are detailed in Extended Data Fig. 7a.
274
275 **Notch activation with ligand-oriented coupling on streptavidin plates**
276 For CHO K1 reporters, on day one, tissue culture 96-well plates (Coastar) were pre-treated with
277 100 µL of streptavidin at 10 µg/mL (VWR) for 1 hour at 37ºC, washed three times with 200 µL
278 DPBS (Corning), and blocked with 100 µL BSA 2% (VWR) for 1 hour at 37ºC. Excess BSA was

279 removed by washing three times with 200 µL DPBS (Corning), and 100 µL of DPBS containing
280 biotinylated DLL4 proteins were coupled to streptavidin for 1 hour at 37ºC (2-fold serial dilutions
281 starting at 50 nM). Non-coupled DLL4 proteins were removed by washing three times with 200
282 µL DPBS. Next, Notch reporter cells in culture were detached with trypsin-EDTA 0.25% (Gibco),
283 and 30,000 cells in α-MEM media (200 µL) were added into individual wells. Assay plates were
284 incubated for 24 hours at 37 ºC, and 5% CO_2. On day two, CHO-K1 Notch1-Gal4 cells were
285 washed with 200 µL DPBS, detached with 30 µL of trypsin-EDTA 0.25%, and 200 µL of α-MEM
286 media added. Cells were resuspended and Notch activation was measured as a function of
287 fluorescence by flow cytometry (BD Accuri C6 plus). CHO-K1 Notch1-Gal4 cells and lacking-
288 ligand wells were used as a negative control. The measurements represent the mean fluorescent
289 intensity as percentage of Notch activation ± S.D. of three biological replicates. Notch activation
290 was reference-subtracted from a well coated with a non-related control protein (PA domain of
291 RNF128).
292
293 For U2OS reporter cells, approximately 5x10E5 cells were plated into 6-well plates (Falcon) and
294 let to adhere overnight at 37 ºC, 5% CO_2 in DMEM media (Cytiva). On day two, media was
295 replaced with serum-free DMEM and cells transfected with luciferase vectors. Cationic lipoplexes
296 were generated for 15 min at room temperature by mixing 10 µL of Lipofectamine 2000
297 (Invitrogen), 2.5µg of Gal4-firefly luciferase reporter, and 50 ng of pRL-TK *Renilla* luciferase
298 vector as internal control (ratio 1:5, Lipo:DNA). On day three, streptavidin plates were coupled
299 with DLL4 ligands like described above using 10-fold serial dilutions starting at 50 nM, and
300 transfected U2OS cells were detached with Trypsin-EDTA, washed with DPBS, and counted in
301 the microscope. Twenty-thousand reporter cells were added to wells using 200 µL of DMEM
302 media containing 2 µg/mL of doxycycline (Sigma) to induce Notch-Gal4 expression. Next,
303 signaling plates were incubated for 24 hours at 37 ºC and 5% CO_2. On day four, luciferase firefly
304 and *Renilla* signals were determined with Dual-Glo luciferase assay system (Promega) using a
305 GloMax luminometer (Promega). A luminescence ratio firefly:*Renilla* was determined for every
306 well and normalized to the signal of a non-related control protein (PA domain of RNF128). Notch
307 activation is represented as the mean fold-change over the control ± S.D. of three independent
308 biological replicates.
309

310 **Kinetics for Notch activation assay**

311 96-well tissue culture plates (Coastar) were pre-coated using ligand-oriented coupling as described
312 above with 50 nM of DLL4 biotinylated variants. CHO-K1 reporter cells were detached with
313 trypsin-EDTA, washed with DPBS, and 200 µL of α-MEM media containing 30,000 cells were
314 added into wells. Notch activation was analyzed as end-points for 0, 4, 8, 12, 16, 20, and 24-hour
315 measurements. Desired time point wells containing CHO-K1 reporter cells were washed once with
316 200 µL DPBS, detached with trypsin-EDTA, and quenched with 200 µL of α-MEM media. Next,
317 reporter cells were resuspended and analyzed by flow cytometry reading the fluorescence of H2B-
318 mCitrine (BD Accuri C6 Plus). Every time point represents the mean fluorescence intensity of
319 Notch activation as percentage ± S.D. of three independent biological replicates. Notch activation
320 was reference-subtracted from a well containing streptavidin, BSA and CHO-K1 cells.

321

322 **Notch activation in co-culture format with HEK293T**

323 On day one, U2OS reporter cells (signal receiver cells) were detached with trypsin-EDTA, washed
324 with DPBS, and 5x10E5 cells were added to 6-well plates (Falcon) for transfection with luciferase
325 reporter vectors. On day two, U2OS cells were transfected as described above. On day three, signal
326 receiver cells were detached with trypsin-EDTA, and 100 µL of DMEM media containing 20,000
327 cells were added to tissue culture 96-well plates (Coastar). In parallel, HEK293T-expressing WT
328 DLL4 or Delta^{MAX} were detached with trypsin-EDTA, counted manually, and dilutions prepared
329 such that 100 µL of DMEM containing 20,000 signal sender cells were added over signal receiver
330 cells (cell ratio 1:1). Doxycycline (Sigma) at 2 µg/mL was used to induce Notch-Gal4 expression.
331 On day four, luciferase firefly and *Renilla* signals were determined with Dual-Glo luciferase assay
332 system (Promega) using a GloMax luminometer (Promega). A luminescence ratio firefly:*Renilla*
333 was determined for every well and normalized to the signal of a well containing U2OS reporter
334 cells and HEK293T non-expressing DLL4 ligands. Notch activation is represented as the mean
335 fold-change over the control ± S.D. of three independent biological replicates.

336

337 **Notch signaling assay using multiple ligand-presentation formats**

338 Notch activation was assayed in different formats (Extended Data Fig. 8a) including (1) non-
339 specific orientation (100 nM of Delta^{MAX} on well, Fig. 3a), (2) ligand-oriented coupling (10 nM
340 of Delta^{MAX} on well, Fig. 3b), (3) magnetic beads coated with biotinylated Delta^{MAX} (ratio 1:20

341 reporter cells:beads, optimization of ratio is detailed in Extended Data Fig. 8d), (4) HEK293T-
342 expressing Delta^{MAX} (ratio 1:1, signal receivers:senders, optimization of ratio can be seen in
343 Extended Data Fig. 8c), and (5) yeast-expressing Delta^{MAX} (ratio 1:10, reporter:yeast,
344 optimization of ratio is detailed in Extended Data Fig. 8b). On day one, U2OS hNotch1-Gal4 cells
345 were detached with trypsin-EDTA, counted in the microscope, and 5x10E5 cells/well transferred
346 to 6-well tissue culture plates (Falcon). On day two, U2OS cells were transfected as described
347 above. On day three, the different activation assays were set up at the same time. For ligand
348 oriented-coupling, streptavidin plates were coated with 10 nM of Delta^{MAX} as described above.
349 For non-specific adsorption, non-biotinylated Delta^{MAX} at 100 nM was coated as described
350 previously. For activation using streptavidin beads coated with biotinylated Delta^{MAX}, 200 mg of
351 streptavidin beads (streptavidin MagneSphere paramagnetic particles, Promega) were washed 3
352 times with 200 µL of DPBS + 0.1% BSA using a magnet (Miltenyi), and combined with 20 µg of
353 biotinylated Delta^{MAX} for 1.5 hours at 4°C. Next, unbound Delta^{MAX} was washed out three times
354 with 200 µL of DPBS + 0.1% BSA, and 100 µL of complexed beads (pre-diluted 1/25 in DPBS)
355 were added to wells. For co-culture activation with HEK293T-expressing Delta^{MAX}, cells were
356 detached with trypsin-EDTA, quenched with DMEM media, washed with DPBS, and 100µL
357 containing 20,000 cells in DMEM were added to wells. For activation with yeast cells expressing
358 Delta^{MAX} on surface, pYAL vector encoding for Delta^{MAX} (N-EGF5) was electroporated
359 previously into yeast cells, and DLL4 expressed in SGCAA as previously described. Delta^{MAX}
360 expression was induced 48 hours before Notch activation assay set up. One hundred microliters of
361 yeast cells (2x10E6 cells/mL) in serum-free DMEM were added to the assay plate. Once all the
362 wells contained the desired activation assays, U2OS reporter cells were detached with trypsin-
363 EDTA, and 20,000 cells in 100 µL of DMEM were added per well. All the conditions were
364 supplemented with 2 µg/mL of doxycycline to induce Notch1-Gal4 expression. The assay plate
365 was incubated for 24 hours at 37°C and 5% CO_2. On day four, media was aspirated off and
366 Luciferase Dual-Glo kit (Promega) used to detect firefly and *Renilla* signals in a luminometer
367 (GloMax, Promega). Negative controls were BSA 0.5% for non-specific absorption, streptavidin
368 and BSA 2% for ligand oriented-coupling, uncoated streptavidin beads for activation with
369 magnetic beads, HEK293T non-expressing DLL4 for co-culture activation, and yeast expressing
370 PDL-1 ECD for co-culture with yeast. The expression of Delta^{MAX} in HEK293T and yeast cells
371 was confirmed by flow cytometry (BD Accuri C6 plus) following staining for 1 hour at 4°C with

372 anti-hDLL4 PE antibody using DPBS + 0.5% BSA, and selection buffer, respectively (Extended
373 Data Fig 8e). Notch activation is represented as the mean fold-change over the corresponding
374 control ± S.D. of three independent biological replicates.
375
376 **Notch inhibition assays with soluble antagonists and WT DLL4 coated plates**
377 For CHO-K1 reporter cells, on day one, biotinylated WT DLL4 was pre-coated in 96-well plates
378 at 50 nM following the same protocol described above. Next, CHO cells were detached with
379 trypsin-EDTA, washed, and diluted at 200,000 cells/mL in α-MEM media. Ten-fold serial
380 dilutions of non-biotinylated DLL4 ligands (N-EGF5) were prepared in DPBS starting at 300 nM.
381 Next, soluble inhibitors were mixed in ratio 1:1 with CHO-K1 200,000 cells/mL stocks for 15 min
382 at room temperature to pre-block Notch receptors. Two hundred microliters of inhibition reactions
383 containing 20,000 reporter cells were added to WT DLL4-coated wells, and plates incubated for
384 24 hours at 37°C and 5% CO_2. When DAPT (gamma-secretase inhibitor, Sigma) and BB-94
385 (ADAM metalloprotease inhibitor, Sigma) were used, stock solutions were prepared at 100 μM in
386 8% DMSO. Appropriate DMSO controls were included to test Notch activation and cell viability.
387 Final DMSO concentration in the experiment was kept below 1%. For comparisons of $Delta^{MAX}$
388 with DAPT and BB-94, soluble inhibitors were serially diluted in DPBS using 9-folds, incubated
389 with CHO reporter cells, and added to wells as described above. On day two, assay plates were
390 washed with 200 μL of DPBS, CHO cells detached with trypsin-EDTA, quenched with 200 μL of
391 α-MEM media, and Notch activation measured by flow cytometry (BD Accuri C6 Plus). The data
392 represents the mean fluorescent intensity as percentage of Notch activation, relative to Notch
393 activation in the absence of inhibitors ± S.D. of three independent biological replicates.
394
395 For U2OS cells, on day one, 5x10E5 cells were plated in 6-well tissue culture plates. On day two,
396 U2OS cells were transfected as described above. On day three, 96-well plates (Coastar) were
397 coated with streptavidin and biotinylated WT DLL4 at 50 nM as described above. Next, U2OS
398 reporter cells were detached with trypsin-EDTA and diluted at 200,000 cells/mL in DMEM media.
399 Ten-fold serial dilutions of soluble DLL4 variants starting at 3,000 nM were prepared in DPBS
400 and used to pre-block reports cells following the same protocol described above. Two-hundred
401 microliters of inhibition reactions were added to 96-well plates pre-coated with biotinylated WT
402 DLL4 ligand at 50 nM, and assay plates incubated for 24 hours at 37°C and 5% CO_2. On day

403 fourth, luciferase signals were measured with Dual-Glo luciferase assay system (Promega) using
404 a GloMax luminometer (Promega). Doxycycline at 2 µg/mL was maintained to ensure binding of
405 soluble inhibitors to Notch-pan receptor. A ratio between firefly and *renilla* luciferase was
406 calculated, and Notch activation normalized to wells where inhibitors were non-added. The data
407 represent fold-change of Notch activation as percentage, relative to Notch activation in the absence
408 of inhibitors ± S.D. of three independent biological replicates.
409
410 **Notch inhibition assay in co-culture format**
411 For inhibition of Notch ligand-expressing cell lines, on day one, U2OS Notch3 reporter cells
412 (signal receivers) were detached with trypsin-EDTA, washed with DPBS, and added to 6-well
413 plates. On day two, U2OS cells were transfected as described above. On day three, signal receiver
414 cells were detached with trypsin-EDTA, and dilutions of 400,000 cells/mL were prepared in
415 DMEM. On the one hand, soluble DLL4 variants were prepared at 6 µM in DPBS, combined in
416 1:1 dilution with signal receiver cells, and incubated for 15 min at RT. On the other hand,
417 HEK293T-expressing WT DLL4, DLL1, JAG1, JAG2 were detached with trypsin-EDTA, washed
418 with DPBS and 200,000 cells/mL stocks prepared in DMEM. One hundred microliters of both
419 signal senders and pre-blocked signal receivers were combined in cell ratio 1:1 and incubated for
420 24 hours at 37°C, and 5% CO_2. On day four, luciferase firefly and *Renilla* signals were determined
421 with Dual-Glo luciferase assay system (Promega) using a GloMax luminometer (Promega).
422 Doxycycline at 2 µg/mL was kept for all the conditions. A luminescence ratio firefly:*Renilla* was
423 determined for every well. Notch activation of each Notch3:ligand pair was normalized to the
424 signal of Notch3 reporters in the presence of HEK293T lacking ligands. Each Notch signaling pair
425 was set at 100% activation and soluble DLL4 treatments were relative to its corresponding pair.
426 The data represent fold-change of Notch activation as percentage, relative to Notch activation in
427 the absence of inhibitors ± S.D. of three independent biological replicates.
428
429 For inhibition of CHO-K1 cells with DAPT and $Delta^{MAX}$, the experiment was set-up following
430 the protocol described above with the exception that CHO-K1 reporters were incubated with
431 HEK293T-expressing WT DLL4 for Notch activation. Three-fold serial dilutions of soluble
432 $Delta^{MAX}$ and DAPT were prepared in DPBS starting at 3 µM. For DAPT, a stock solution of 100
433 µM in 8% DMSO was prepared before serial dilutions in DPBS. Appropriate DMSO controls were

434 also assayed for cytotoxicity. Final DMSO concentration in the wells was maintained below 1%.
435 Thirty thousand signal senders and pre-blocked signal receivers (100 µL each) were incubated for
436 24 hours at 37°C and 5% CO_2 before analysis by flow cytometry. Maximum Notch activation
437 (100%) was set in the absence of soluble inhibitors and normalized to wells containing CHO-K1
438 cells and HEK293T lacking expression of WT DLL4. Mean fluorescence intensity is represented
439 as percentage relative to Notch activation in the absence of inhibitors ± S.D. of three independent
440 biological replicates.
441
442 **Co-culture assays for T-cell activation and proliferation**
443 Functional assays for human $CD8^+$ T cells were performed in co-culture with K562 cells
444 expressing human CD32 (K32 cells) generated as described before[5]. Briefly, cells were γ-
445 irradiated (100Gy) and washed twice with PBS before being loaded with OKT3 (0.0125-
446 0.5µg/mL, BioXcell) antibody at RT for 10 min. Human $CD8^+$ T cells were negatively isolated
447 from PBMC and labeled with 5µM of Cell Trace Violet (Invitrogen) according to manufacturer's
448 specifications. Next, $CD8^+$ T cells were co-cultured with K32 cells at ratio 1:10 (T cell: K32). The
449 frequency of proliferating T cells was determined after 96 hours by flow cytometry using a
450 CytoFLEX II (Beckman Coulter). Zombie Green (Biolegend) was used for life/dead cell staining
451 to discard dead cells from the analysis. A set of samples were additionally incubated with Golgi
452 stop (BD) at 0.5 µL/well for 5 hours and washed with PBS for detection of intracellular IFNγ using
453 anti-hIFNγ APC antibody (Biolegend). The frequency of IFNγ positive cells was analyzed by flow
454 cytometry (CytoFLEX II, Beckman Coulter). Dead cells were excluded from the analysis by
455 staining with Zombie green (Biolegend). The data represents the mean percentage of proliferating
456 T cells or $IFN\gamma^+$ T cells ± S.E.M of four independent biological replicates.
457
458 **Quantitative Real-time PCR**
459 Human $CD8^+$ T cells were co-cultured with K32-DLL4 cells for 96 hours and positively enriched
460 by MACS column (Invitrogen Kit). Total RNA was isolated from $CD8^+$ T cells using TRIzol (Life
461 Technologies). Reverse transcription reaction was performed using Verso cDNA Synthesis Kit
462 (Thermo Scientific). Quantitative PCR reactions were prepared by using Bio-Rad SYBR green
463 master mix and performed on an Applied Biosystems thermocycler (7900 HT). Relative expression
464 was calculated using the ΔΔCt method and normalized to β2M levels. The data represents the mean

465 quantity of mRNA (in-fold) for different T cell markers ± S.E.M of four independent biological
466 replicates. Pair primers used were:
467 Human β2-Microglobulin
468 Forward: 5'-ATGAGTATGCCTGCCGTGTGA
469 Reverse: 5'-GGCATCTTCAAACCTCCATG
470 Human IFNγ
471 Forward: 5'-GACCAGAGCATCCAAAAGAG
472 Reverse: 5'-GGACATTCAAGTCAGTTACCGAATA
473 Human Granzyme B
474 Forward: 5'-CCCTGGGAAAACACTCACACA
475 Reverse: 5'-GCACAACTCAATGGTACTGTCG)
476 Human Hes-4
477 Forward: 5'-ACGGTCATCTCCAGGATGT
478 Reverse: 5'-CGAGCGCGTATTAACGAGAG)
479
480 **Immunoblot Analysis**
481 For detection of Notch activation in $CD8^+$ T cells, following co-culture with K32 cell lines, $CD8^+$
482 T cells were positively enriched by Magnisort Human $CD8^+$T cell positive selection Kit
483 (Invitrogen). Nuclear fraction was isolated using NE-PER Nuclear and Cytoplasmic extraction kit
484 (ThermoFisher). Equal protein amounts of nuclear cell lysates were run on 4-20% gradient Tris-
485 glycine gels (Novex-Invitrogen), transferred to PVDF membranes using an iBlot Gel Transfer
486 Device (ThermoFisher), and immunoblotted with antibodies anti-cleaved Notch1 (Val1744 rabbit
487 mAb, Cell Signaling Technology, 1:1,000), anti-Notch2 (D76A6 rabbit mAb, Cell Signaling
488 Technology, 1:1,000), and anti-β Actin (mouse mAb, Sigma, 1:20,000). Secondary antibodies anti-
489 IgG (anti-rabbit or anti-mouse, GE Healthcare, 1:5,000) conjugated to horseradish peroxidase
490 (HRP) were used for detection of proteins using ECL Western Blot Substrate Reagent (Thermo
491 Fisher Scientific). Images were acquired using a Chemidoc Imaging System and analyzed with
492 Image-Lab software (Bio-Rad).
493
494 For Notch activation in U2OS and MCF-7 cells, WT DLL4 and $Delta^{MAX}$ biotinylated ligands
495 were immobilized at 50 nM in 6-well streptavidin-coated plates following a scaled up protocol of

496 the one described before. After 24 hours of stimulation, cells were lysed in Laemmli serum buffer
497 (40% glycerol, 4% SDS, 250 mM Tris-HCl, 0.02% bromophenol blue, and 20% β-
498 mercaptoethanol). Cell lysates were heated at 100°C for 5 min, centrifuged at 21,000*xg* for 10 min
499 at 4°C, and supernatants stored at -20°C. Proteins were separated by SDS-PAGE (12% Mini-
500 PROTEAN TGX Precast Protein Gels, Bio-Rad) and transferred to PVDF membranes using an
501 iBlot2 Gel Transfer Device (Thermo Fisher Scientific). The membranes were blocked in 3% BSA
502 + 0.1% TBS-Tween. Primary antibodies were anti-cleaved Notch1 (Val1744 rabbit mAb, Cell
503 Signaling Technology, 1:1,000), and β-Actin (rabbit pAb, Cell Signaling Technology, 1:1,000).
504 Secondary antibody anti-Rabbit IgG conjugated to HRP (Goat mAb, Vector Laboratories, 1:8,000)
505 was used for detection of proteins using SuperSignal West Pico PLUS Chemiluminescent
506 Substrate (Thermo Fisher Scientific). Images were acquired using an Amersham Imager 600 (GE
507 Healthcare), and contrast adjusted with a curves layer.
508
509 **References**
510 1. Sprinzak, D. *et al.* Cis-interactions between Notch and Delta generate mutually exclusive
511 signalling states. *Nature* **465**, 86–90 (2010).
512 2. Malecki, M. J. *et al.* Leukemia-Associated Mutations within the NOTCH1 Heterodimerization
513 Domain Fall into at Least Two Distinct Mechanistic Classes. *Mol Cell Biol* **26**, 4642–4651 (2006).
514 3. Luca, V. C. *et al.* Notch-Jagged complex structure implicates a catch bond in tuning ligand
515 sensitivity. *Science* **355**, 1320–1324 (2017).
516 4. Luca, V. C. *et al.* Structural basis for Notch1 engagement of Delta-like 4. *Science* **347**, 847–853
517 (2015).
518 5. Maus, M. V. *et al.* Ex vivo expansion of polyclonal and antigen-specific cytotoxic T
519 lymphocytes by artificial APCs expressing ligands for the T-cell receptor, CD28 and 4-1BB. *Nat*
520 *Biotechnol* **20**, 143–148 (2002).
521
522
523
524
525
526

527 **EXTENDED DATA FIGURES**

528

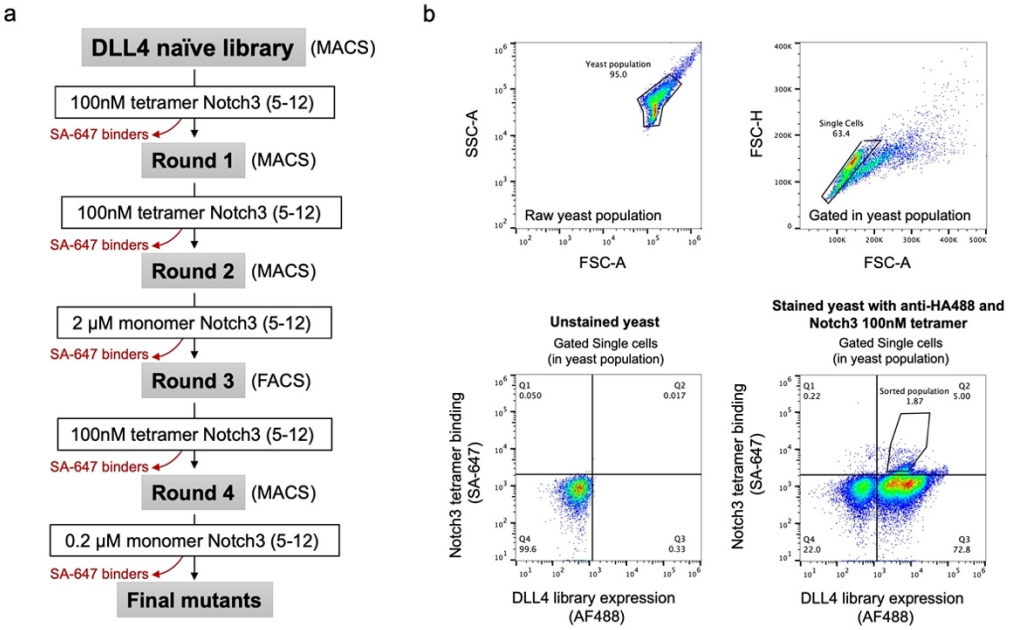

529

530 **Extended Data Fig 1. Selection strategy for isolation of high-affinity DLL4 populations.** (**A**)
531 Flow chart depicting the selection strategy used to isolate high-affinity DLL4 variants. Red arrows
532 and text indicate negative selections. (**B**) Gating strategy for sorting high-affinity binders to
533 Notch3.

534

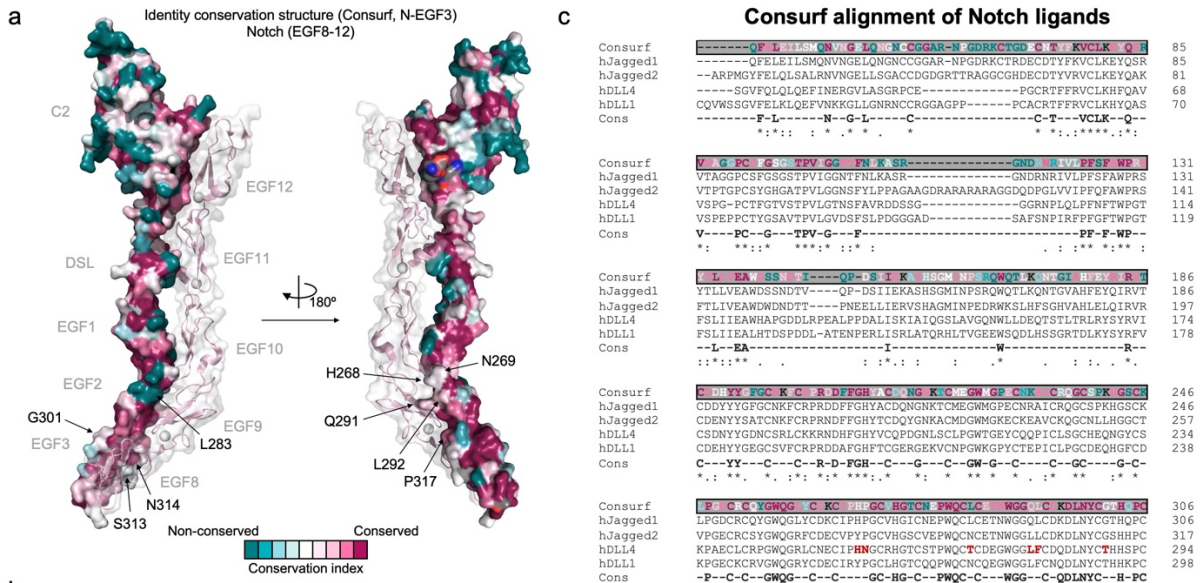

	JAG1	JAG2	DLL4	DLL1
JAG1	100.0	62.1	44.6	44.7
JAG2	62.1	100.0	44.2	46.6
hDLL4	44.6	44.2	100.0	59.7
hDLL1	44.7	46.6	59.7	100.0

Extended Data Fig 2. Conservation analysis of Site 3 library positions in activating Notch ligands. (**A**) A structural model depicting amino acid conservation in DLL1, DLL4, Jag1, and Jag2 residues was generated in Consurf using rat JAG1 as a template (PDB ID: 5UK5). (**B**) Identity matrix indicating the sequence identity between human Notch ligands. (**C**) Sequence alignment depicting conservation at each residue position. Residues mutated in the DLL4 mutant library are highlighted in red.

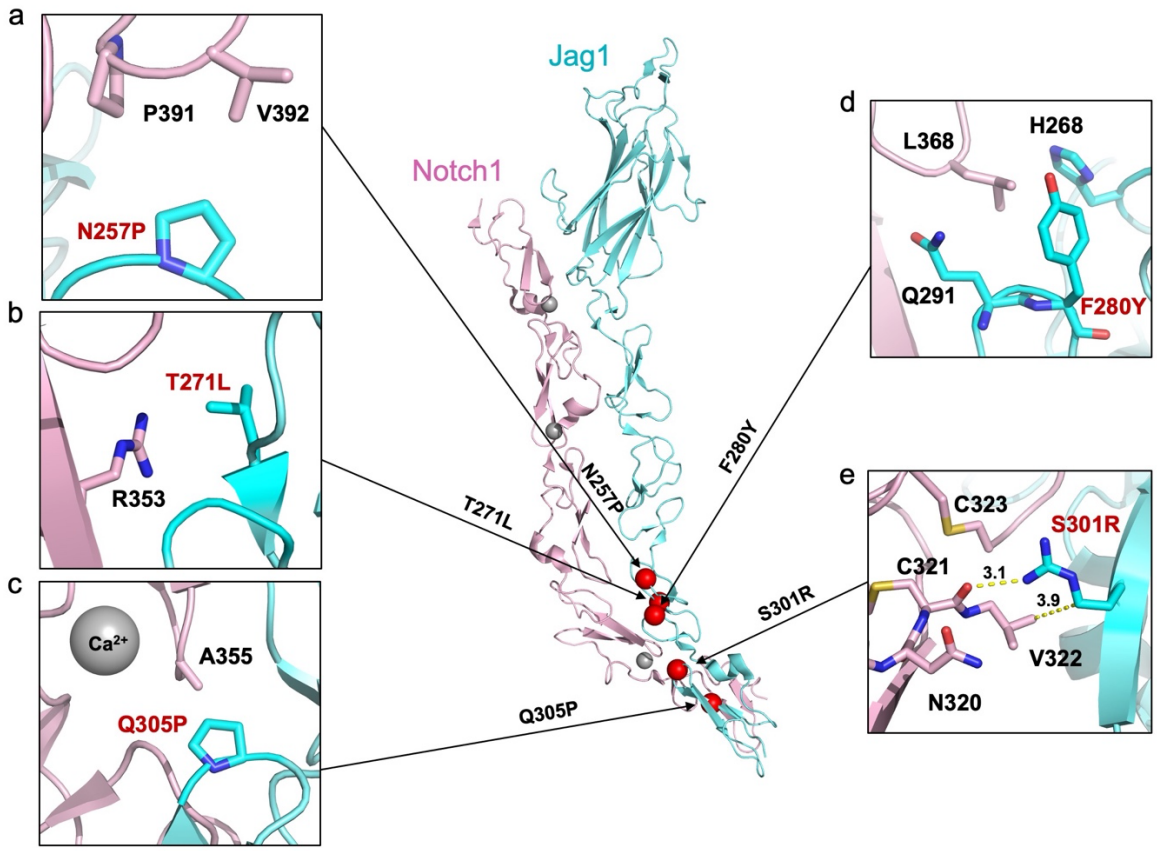

554

555 **Extended Data Fig 3. Mutational analysis of evolved DLL4 Site 3 over Jagged1:Notch1**
556 **structure.** Cartoon representation showing the structural context of DLL4.v2 mutants in a model
557 of the rat Jag1-Notch1 complex (PDB ID:5UK5). (**A**), (**B**), (**C**), (**D**), and (**E**) are zoom panels
558 depicting the residues that surround the mutated position. Numbers and dashes in **(E)** are inter-
559 atomic distances atoms measured in angstroms.

560

561

562

563

564

565

566

567

568

569

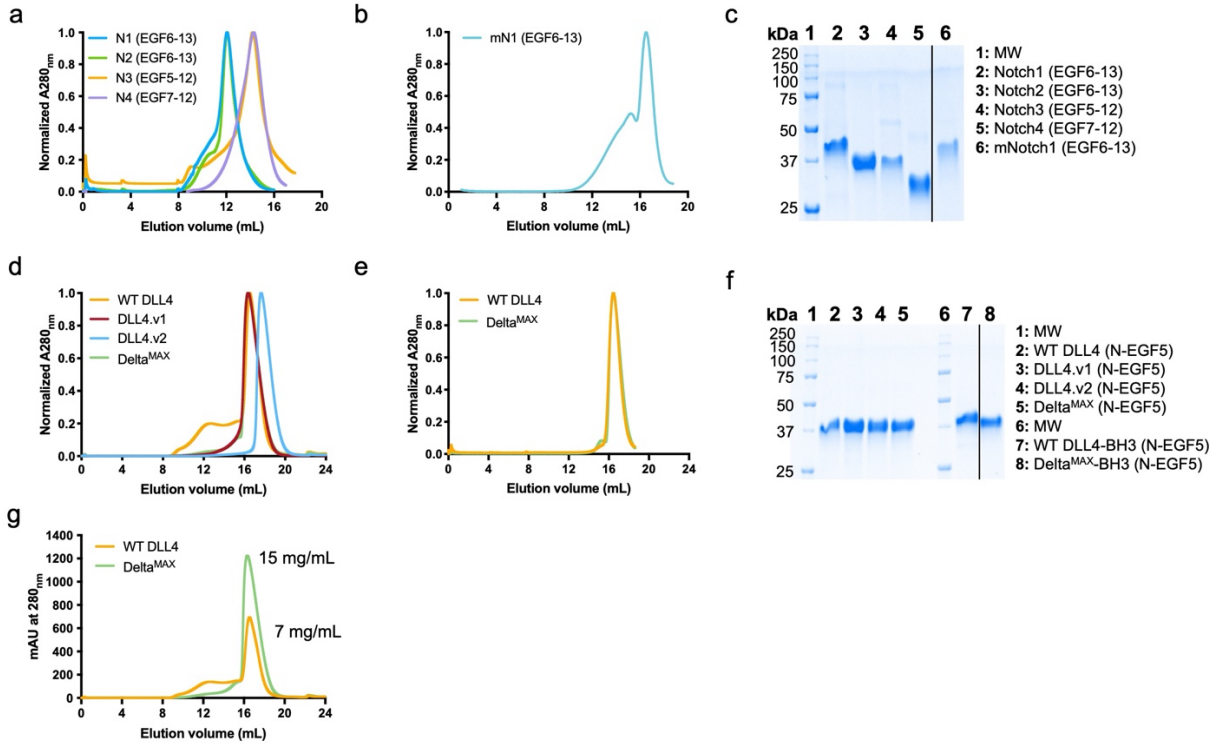

Extended Data Fig 4. Purification of Notch and DLL4 fragments for SPR studies and signaling assays. (A-B) SEC chromatograms from the purification of the ligand-binding regions of human Notch1-4 **(A)** and murine Notch1 **(B)**. All proteins were purified by Ni-NTA followed by size exclusion chromatography using a Superdex S75 column. **(C)** SDS-PAGE gels showing the purity and molecular weight of each Notch construct. (**D**) SEC chromatograms from the purification of DLL4, DLL4.v1, DLL4.v2, and Delta^{MAX} proteins. All proteins were purified by Ni-NTA followed by size exclusion chromatography using a Superdex S200 column. **(E)** SEC chromatograms from the purification of C-termini biotinylated WT DLL4 and Delta^{MAX} proteins. **(F)** SDS-PAGE gels showing the purity and molecular weight of each DLL4 construct. **(G)** SEC chromatograms from 1L protein preps were overlaid to highlight the increased yield of recombinant Delta^{MAX} compared to WT DLL4.

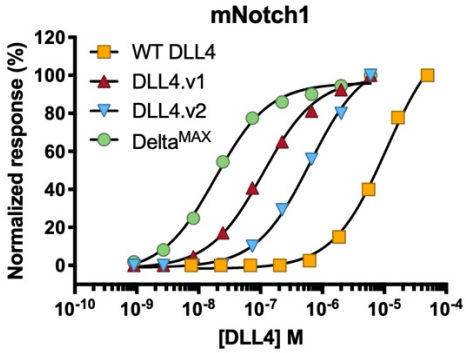

Extended Data Fig 5. SPR binding assays for mNotch1. SPR binding isotherms were fitted to a 1:1 binding model to determine the binding affinity between mNotch1(6-13) and each DLL4 variant.

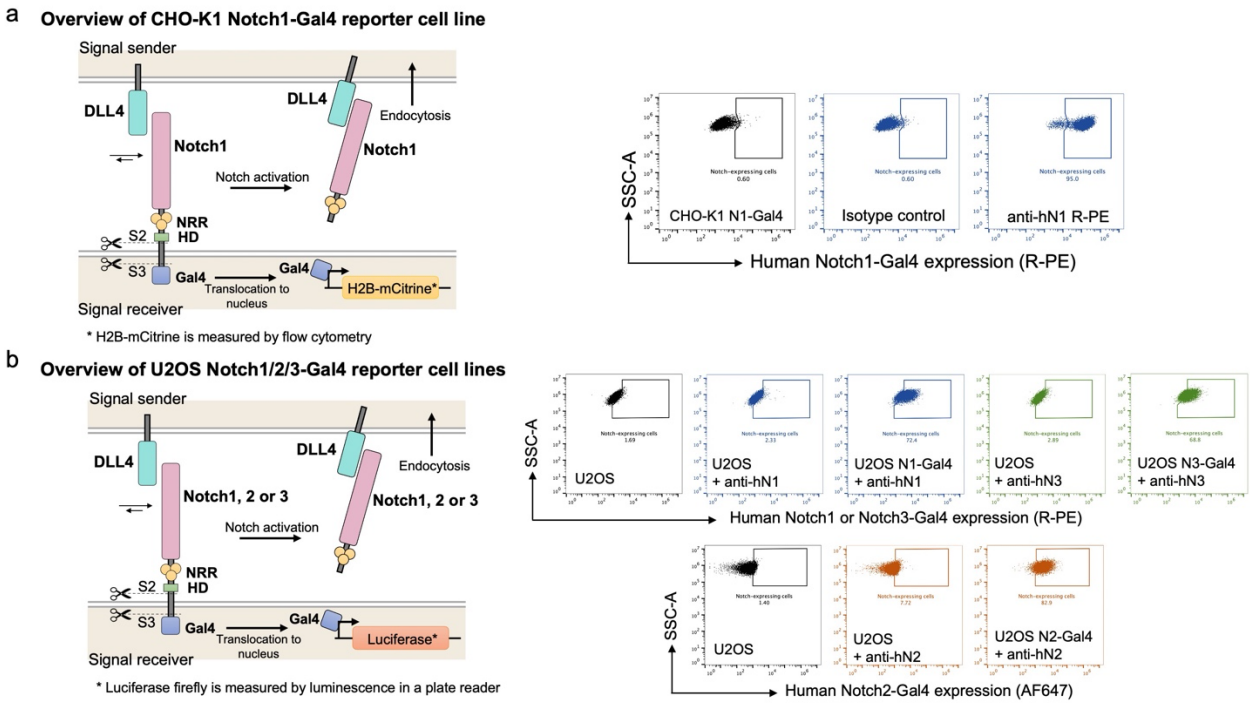

Extended Data Fig 6. Notch reporter cell lines used in this study. Cartoon schematics describing the fluorescent **(A)** and luminescent **(B)** Notch-Gal4 reporter systems used for signaling assays. Flow cytometry dot plots depict the staining of each cell line with Notch-specific antibodies to detect surface expression.

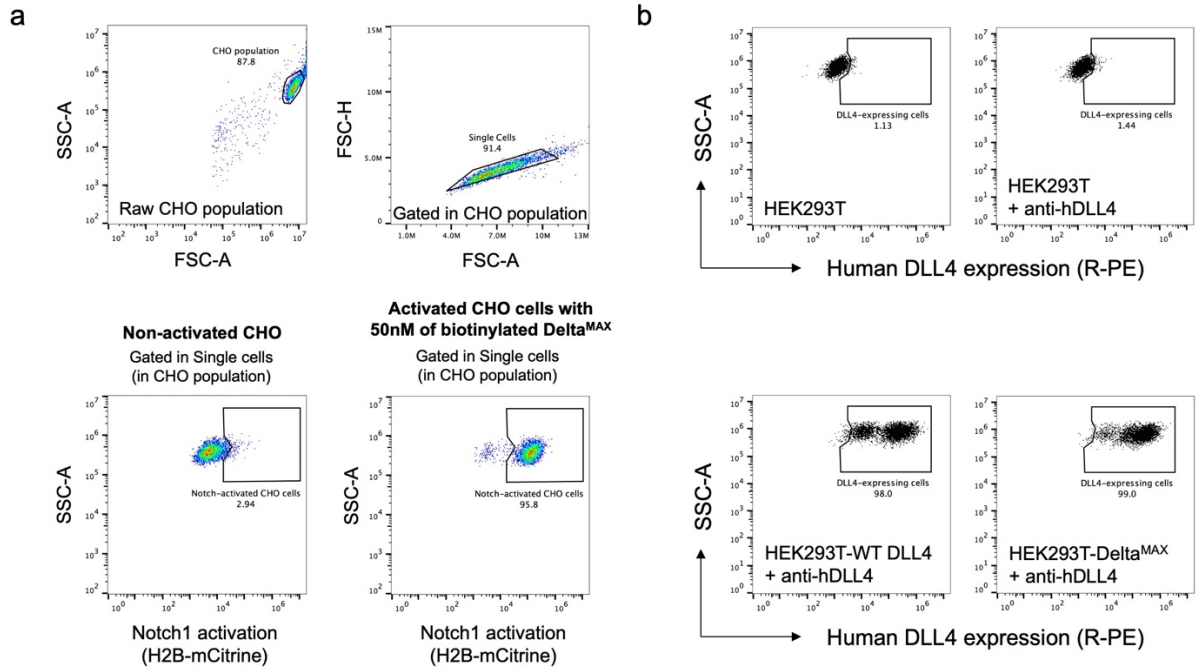

Extended Data Fig 7. Gating strategy for Notch activation assays using CHO-K1 and detection of DLL4 expression in HEK293T stable cell lines. (**A**) DLL4 variants were non-specifically adsorbed to 96-well tissue culture plates or immobilized to streptavidin plates. Next, CHO-K1 Notch1-Gal4 cells were added to plates and Notch activation was measured by flow cytometry. The gating strategy to quantify Notch1 activation based on expression of H2B-mCitrine using CHO reporter cells is detailed. HEK293T were transduced to generate stable cell lines expressing WT DLL4 or Delta^{MAX} and sorted to normalize the expression of DLL4. (**B**) Expression of WT DLL4 and Delta^{MAX} on HEK293T was analyzed with anti-hDLL4 PE antibody using flow cytometry. The sorted cell lines were used for Notch activation assays in co-culture with Notch1, Notch2, and Notch3-U2OS luciferase reporters.

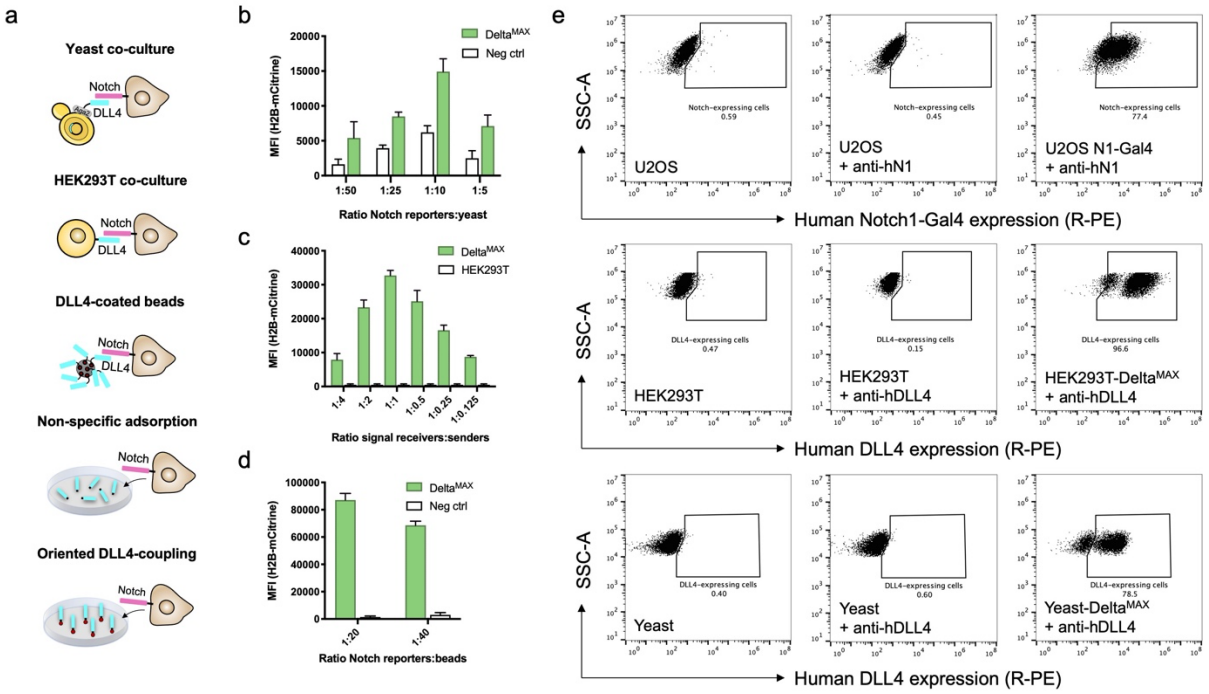

Extended Data Fig 8. Optimization for all-in-one assay using Delta^{MAX}. (**A**) Cartoon representation of different ligand-presentation formats. (**B**) Yeast expressing Delta^{MAX} (N-EGF5) were co-cultured with CHO-K1 reporter cells for 24h at different ratios and fluorescence was measured by flow cytometry. (**C**) HEK293T cells expressing Delta^{MAX} were co-cultured with Notch1 reporter cells at various ratios for 24h and Notch activation was measured by flow cytometry. (**D**) Magnetic beads were pre-coated with biotinylated Delta^{MAX} and co-cultured with CHO K1 reporter cells at ratios of 1:20 or 1:40 to stimulate Notch activation. (**E**) Flow cytometry dot plots depict the expression level of Notch1 and Delta^{MAX}.

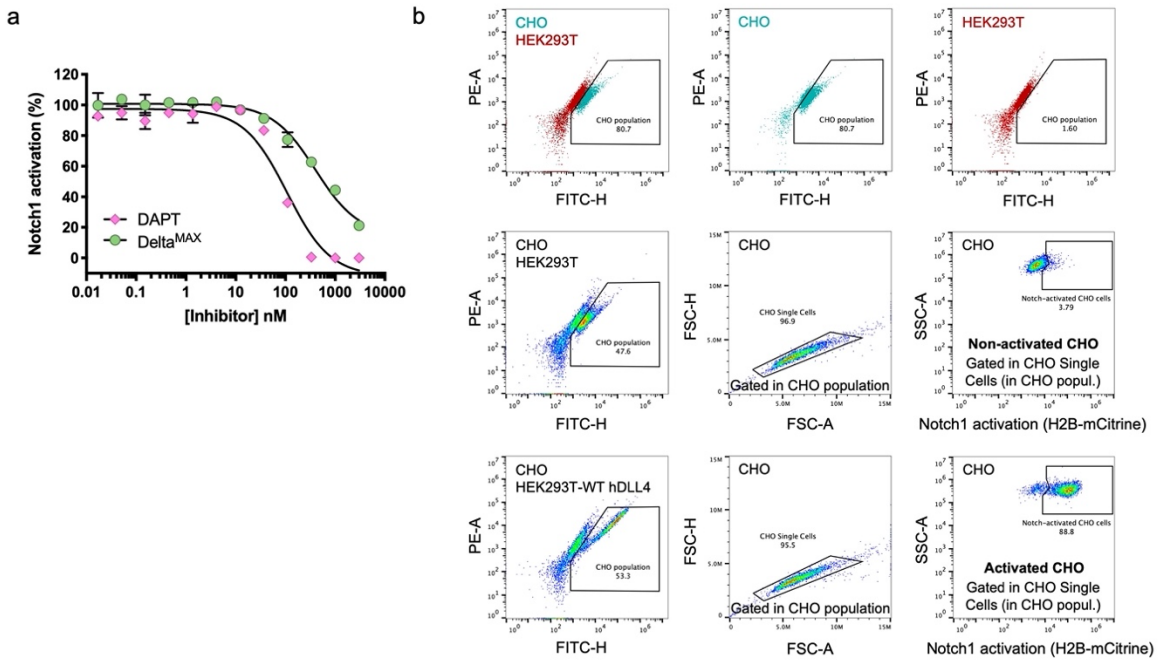

Extended Data Fig 9. Co-culture inhibition using CHO-K1 cells, DAPT, or Delta^{MAX} as soluble antagonists. (**A**) Dose-titration assay comparing the inhibition potency of DAPT and Delta^{MAX}. Fluorescent Notch1 reporter cells were cultured in a 1:1 ratio with HEK293T cells stably expressing WT DLL4. (**B**) Summary of the gating strategy used for flow cytometry to differentiate between HEK293T and CHO cell signals. The basal expression of H2B-mCitrine in CHO cells was used as a criterion to distinguish between cell types. Notably, the population identified in the middle and bottom panels (Notch1 reporter CHO cells) corresponds to approximately 50% of the total cells, which is consistent with a 1:1 ratio of CHO cells to 293T cells.

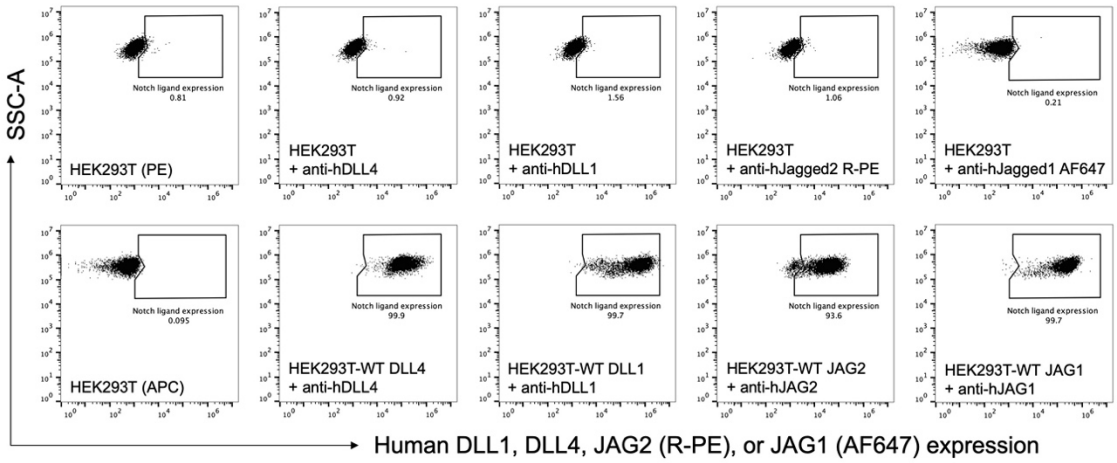

Extended Data Fig 10. Detection of Notch ligands expressed on HEK293T stable cell lines by flow cytometry. HEK293T stable cells lines expressing WT DLL4, DLL1, JAG1, or JAG2 were stained with specific antibodies targeting the ECDs of each Notch ligand and measured by flow cytometry. The expression of Notch ligands, as well as sequencing results, validated these stable cell lines.